DMD Fast Forward. Published on July 22, 2014 as DOI: 10.1124/dmd.114.059204
This article has not been copyedited and formatted. The final version may differ from this version.

DMD #59204

BIOSYNTHESIS OF DRUG METABOLITES AND QUANTITATION USING NMR SPECTROSCOPY FOR USE IN PHARMACOLOGICAL AND DRUG METABOLISM STUDIES

Gregory S. Walker, Jonathan N. Bauman, Tim F. Ryder, Evan B. Smith, Douglas K. Spracklin, and R. Scott Obach

Biotransformation Group

Pharmacokinetics, Dynamics, and Metabolism

Pfizer Inc.

Groton, CT

DMD Fast Forward. Published on July 22, 2014 as DOI: 10.1124/dmd.114.059204
This article has not been copyedited and formatted. The final version may differ from this version.

Running Title: BIOSYNTHESIS OF METABOLITES FOR USE IN PHARMACOLOGICAL STUDIES

Number of Tables: 0

Number of Figures: 12

Number of Words in:

Abstract: 219

Introduction: 749

Discussion: 1429

Address Correspondence to either:

Gregory S. Walker (gregory.s.walker@pfizer.com) or R. Scott Obach (r.scott.obach@pfizer.com)

Pfizer Inc.

Eastern Point Rd.

Groton, CT, USA 06340

Abbreviations: HPLC (high pressure liquid chromatography), HSQC (heteronuclear single quantum coherence), HMBC (heteronuclear multiple bond correlation), COSY (correlation spectroscopy), TOCSY (total correlation spectroscopy), NOE (nulear overhauser effect), DMSO-d_6 (hexadeutarated dimethylsulfoxide), PDA (photo diode array), CH_3CN (acetonitrile) TIC (total ion chromatogram), XIC (extracted ion chromatogram), NMR (nuclear magnetic resonance), qNMR (quantitative nuclear magnetic resonance)

DMD Fast Forward. Published on July 22, 2014 as DOI: 10.1124/dmd.114.059204
This article has not been copyedited and formatted. The final version may differ from this version.

ABSTRACT

The contribution of drug metabolites to the pharmacological and toxicological activity of a drug can be important; however, for a variety of reasons metabolites can frequently be difficult to synthesize. To meet the need of having samples of drug metabolites for further study, we have developed biosynthetic methods coupled with quantitative NMR spectroscopy (qNMR) to generate solutions of metabolites of known structure and concentration. These quantitative samples can be used in a variety of ways when synthetic sample is unavailable, including pharmacological assays, standards for *in vitro* work to help establish clearance pathways and/or as analytical standards for bioanalytical work to ascertain exposure, among others. In this manuscript five examples of metabolite biosynthesis and qNMR are illustrated. The types of metabolites include one glucuronide and four oxidative products. Concentrations of the isolated metabolite stock solutions ranged from 0.048 to 8.3 mM, with volumes from approximately 0.04 to 0.150 mL in hexadeutarated dimethylsulfoxide (DMSO-d_6). These specific quantified isolates were used as standards in the drug discovery setting as substrates in pharmacology assays, for bioanalytical assays to establish exposure and in variety of routine ADME assays like protein binding and determining blood to plasma ratios. The methods used to generate these materials are described in detail with the objective that these methods can be generally used for metabolite biosynthesis and isolation.

DMD Fast Forward. Published on July 22, 2014 as DOI: 10.1124/dmd.114.059204
This article has not been copyedited and formatted. The final version may differ from this version.

INTRODUCTION

A majority of drugs undergo metabolism as their main mechanism of clearance. A variety of enzymes catalyze oxidation, reduction, hydrolysis, and conjugation reactions (Parkinson et al, 2013). Delineation of the metabolic pathways of new drug candidates is expected by regulatory agencies. An understanding of the metabolism of new chemical entities can aid in drug research to design compounds with improved pharmacokinetic properties (i.e. low clearance, low first pass metabolism, half-lives suitable for convenient dosing).

The metabolites of drugs and new drug candidates can be important for several reasons. First, since metabolism can be a major clearance mechanism for a new drug, structural knowledge of the main metabolites permits an informed inquiry into what drug metabolizing enzymes may be responsible for clearance. Knowledge of enzymes responsible for clearance can permit an understanding of the potential for interpatient variability in pharmacokinetics, drug-drug interactions, and impact of genetic polymorphisms on drug and metabolite exposure (Zhang, et al., 2007). Second, drug metabolites can possess similar binding potency to the same pharmacological target as the parent drug, and thus could contribute to clinical effect (Obach, 2013). Knowledge of potency, pharmacokinetics, and target tissue distribution of active metabolites is important for establishing the pharmacokinetic-pharmacodynamic relationship and dosing regimen. It can also be possible that an active metabolite can be a drug itself; three common antihistamines, fexofenadine, desloratadine, and cetirizine, are all active metabolites of first generation antihistamines (terfenadine, loratadine, and hydroxyzine, respectively) with improvements in clinical profiles. Third, drug metabolites have been subjected to increased focus over the past decade because of their potential to be responsible for toxicity (i.e. the "MIST" issue; Baillie, et al., 2002; Smith and Obach, 2009; ICH, 2009). During the

DMD Fast Forward. Published on July 22, 2014 as DOI: 10.1124/dmd.114.059204
This article has not been copyedited and formatted. The final version may differ from this version.

development of a new drug, an assurance is needed that metabolites to which humans are exposed have been acceptably tested for toxic potential. Usually this is assessed by virtue of metabolite exposure in laboratory animals following administration of the parent drug.

Because of these points, it is important to obtain authentic standards of human drug metabolites. These standards can be used to test for target activity or to construct calibration curves for measurement of drug concentrations. However, chemical synthesis of metabolites can be challenging. A metabolite of interest can be one structure of many regiochemical and/or stereochemical possibilities, requiring the synthesis of several isomers to establish which possibility is correct. As an alternative to chemical synthesis, microbiological and biomimetic methods have been described for the generation of drug metabolites (Bernadou and Meunier, 2004; Li, et al., 2009). However, use of these methods requires proof that the correct metabolite isomer is being made by the system employed.

When drug metabolizing enzymes from human or laboratory animal species are employed as the biological system to prepare an authentic standard of a metabolite, there is greater assurance that the truly desired metabolite is being made (Li, et al., 2009). However, a challenge of such biological reagents is the generation of enough product to permit isolation of enough material to weigh. These techniques can produce the desired metabolites, but generally only in the tens of microgram range (5-500 nmoles). It is not feasible to accurately weigh isolates of this magnitude. However quantitative NMR (qNMR) can be used to provide concentrations of isolated metabolite in this weight range (Espina, et al. 2009, Vishwanathan et al. 2009, Walker, et al., 2011). While NMR is typically thought of as a qualitative technique that yields structural information, the quantitative nature of NMR has long been utilized in the field of natural products (Pauli et al., 2012). What separates NMR from other spectroscopic

DMD Fast Forward. Published on July 22, 2014 as DOI: 10.1124/dmd.114.059204
This article has not been copyedited and formatted. The final version may differ from this version.

techniques (e.g. MS, UV/VIS) as a quantitative method is the uniform response to hydrogen atoms. This enables several different strategies using internal and external standards to quantitate unknown organic compounds without a qualified reference standard.

In this paper, we describe methods for making and isolating metabolites in quantities from 5 to 500 nmole. Metabolites are generated using liver microsomes in incubation volumes of tens of milliliters and isolated using HPLC. The residues in fractions containing metabolites of interest are analyzed by qNMR to yield small volumes (~50 -150 µL) of metabolite solutions of known concentrations (typically 0.1 to 5 mM) in DMSO-d_6. These solutions can then be used as stock solutions from which dilutions can be made to test for *in vitro* pharmacological activity, used as standards for calibration curves or other drug metabolism studies. The methods are illustrated using five examples (Figure 1) and the uses of these biosynthesized standards are briefly described.

DMD Fast Forward. Published on July 22, 2014 as DOI: 10.1124/dmd.114.059204
This article has not been copyedited and formatted. The final version may differ from this version.

MATERIALS and METHODS

Materials. Compounds A ((3*S*)-3-amino-1-hydroxy-6-phenoxy-3,4-dihydroquinolin-2(1*H*)-one), B 4-(azetidin-1-yl)-3-[5-(4-ethylphenyl)-1-methyl-1*H*-pyrazol-4-yl]-1-methyl-1*H*-pyrazolo[3,4-*d*]pyrimidine, C *N*-(2,4-di-*tert*-butyl-5-hydroxyphenyl)-4-oxo-1,4-dihydroquinoline-3-carboxamide and D (ethyl 1-[({[3-(dimethylcarbamoyl)-4-({[4'-(trifluoromethyl)biphenyl-2-yl]carbonyl}amino)phenyl]acetyl}oxy)methyl]-1,3-dihydro-2-benzofuran-1-carboxylate) were synthesized by Pfizer. Atazanavir (methyl {(5S,10S,11S,14S)-11-benzyl-5-tert-butyl-10-hydroxy-15,15-dimethyl-3,6,13-trioxo-8-[4-(pyridin-2-yl)benzyl]-2-oxa-4,7,8,12-tetraazahexadecan-14-yl}carbamate) was obtained from Sequoia Research Products (Pangbourne, UK). Recombinant heterologously expressed CYP3A5 (123 pmol/mg microsomal protein) was obtained from Panvera (Madison, WI). NADPH and UDPGA were from Sigma (St. Louis, MO). Human and female dog liver microsomes as well as dog intestinal microsomes were purchased from BD-Gentest (Woburn, MA). The human liver microsomes consisted of a pool of 50 male and female donors. All deuterated solvents were purchased from Cambridge Isotope Laboratories, Inc. (Tewksbury, MA).

Equipment. The following equipment was utilized in these preparations unless otherwise noted: Jouan Model CT422 centrifuge (Saint-Herblain, France), Beckmann-Coulter Spinchron DLX centrifuge (Brea, CA), Genevac Evaporator (Genevac, Valley Cottage, NY), Jasco PU-980 HPLC pump (Jasco Analytical Instruments, Easton, MD), AB Sciex Triple TOF 5600 mass spectrometer (Framingham, MA) with a Shimadzu CBM-20A controller (Shimadzu USA, Columbia, MD), LC-20ADXR pumps (Shimadzu USA, Columbia, MD), CTC PAL Autosampler (Leap Technologies, Carrboro, NC) and Agilent 1100 PDA (Santa Clara, CA), Thermo-Fisher HPLC-MS containing Surveyor quaternary HPLC, Surveyor PDA detector and LTQ mass

spectrometer (Thermo Fisher, Wilmington, DE), Gilson FC-204 fraction collector (Gilson, Middletown, WI), Shimadzu semi preparative HPLC system containing a SiL-HTC autosampler, two LC-20AD solvent pumps, an SPD-M20A diode array detector, and a FRC-10 fraction collector (Shimadzu USA, Columbia, MD), Nexus II dry box (Vacuum Atmospheres, Hawthorne CA), and Bruker Avance 600 MHz NMR Spectrometer controlled by Topspin V3 with a TCI Cryo probe (1.7 or 5 mm) (Bruker BioSpin Corporation, Billerica, MA). Polypropylene microtiter plates were from Arctic White (Bethlehem, PA).

General Method 1. In general method 1, parent compound (typically 10-100 μM) is incubated in an *in vitro* system containing a source of drug metabolizing enzyme and cofactors necessary to effect the biotransformation of interest. The reaction volume typically ranges between 10 and 100 mL and is carried out in an Erlenmeyer flask in a shaking water bath at 37^{o} C. At the end of the incubation, the reaction is terminated by addition of CH_3CN (1-4 volumes) and the mixture spun in a centrifuge to remove the precipitant. The supernatant is subject to vacuum centrifugation to remove organic solvent and to the remaining supernatant is added aqueous formic acid to a total volume of 25-150 mL. This mixture is subject to centrifugation at 40000 x *g* and the resulting clear supernatant is applied to an HPLC column through an HPLC pump. After the material is applied, the column is moved to a gradient HPLC-MS system coupled to a fraction collector, and an HPLC solvent program is applied to elute the product(s) of interest. Fractions containing the metabolite(s) of interest are combined and the solvent removed by vacuum centrifugation. Residues are dissolved in DMSO-d_6 for NMR analysis.

General Method 2. In general method 2, incubations are carried out as in Method 1. Following centrifugation of terminated incubation mixtures as above, the supernatants are transferred to clean 50 mL polypropylene centrifuge tubes and concentrated to dryness in a Genevac vacuum

centrifuge. The residues in each tube are reconstituted 10% CH_3CN in water (<2 mL). The reconstituted samples are combined in a 2 mL HPLC vial and are injected onto a HPLC semipreparative system as multiple 300 µL injections collecting the post column effluent on a fraction collector. Fractions containing the metabolite(s) of interest are combined and the solvent removed by vacuum centrifugation. Residues are dissolved in DMSO-d_6 for NMR analysis.

Example A: Biosynthesis of Compound A Glucuronide Using Method 1. Compound A (50 µM) was incubated with human liver microsomes (2 mg/mL) containing 25 µg/mL alamethicin, 5 mM $MgCl_2$, and 5 mM UDPGA in a total volume of 20 mL KH_2PO_4 (100 mM, pH 7.4). The incubation was conducted in a 250 mL Erlenmeyer flask in a shaking water bath maintained at 37^o C for 1 hr. At the end of the incubation, 20 mL CH_3CN was added, the mixture was transferred to two 50 mL polypropylene conical tubes and vigorously mixed on a vortex mixer. The tubes were spun in a Jouan centrifuge at 1700 x *g* for 5 min and the supernatant was transferred to new 50 mL polypropylene conical tubes. The tubes were subjected to vacuum centrifugation in a Genevac evaporator set at the HPLC mixture setting for approximately 1 hr to remove the CH_3CN. To the remaining solution was added water to a total volume of ~100 mL and formic acid (1 mL). This mixture was subjected to centrifugation in a Beckmann centrifuge at 40000 x *g* for 30 min to clarify the supernatant. The supernatant was transferred to a 100 mL graduated cylinder and directly applied onto a Varian Polaris C18 column (4.6 x 250 mm; 5 µm particle size) through a Jasco HPLC pump at a flow rate of 0.8 mL/min. Following application of the 100 mL, another ~10 mL of 0.1% formic acid was pumped onto the column to ensure that the HPLC lines were cleared of the supernatant.

DMD Fast Forward. Published on July 22, 2014 as DOI: 10.1124/dmd.114.059204
This article has not been copyedited and formatted. The final version may differ from this version.

The HPLC column was then transferred to a Thermo LTQ HPLC-UV-MS system with the mass spectrometer operated in the positive ion mode. The effluent was split between the mass spectrometer and a Gilson fraction collector at a ratio of approximately 1:15. The mobile phase used consisted of 0.1% formic acid (mobile phase A) and CH_3CN (mobile phase B) at a flow rate of 0.8 mL/min. The mobile phase composition commenced at 95%A/5%B, was held at that composition for 5 min, followed by a linear gradient to 50%A/50%B at 25 min, a second gradient to 20%A/80%B at 30 min, held at this composition for 5 min, then reequilibrated at initial conditions for 10 min. The mobile phase program and data collection was started by making a dummy injection of water from the autosampler. Fractions were collected every 20 sec into a wide-welled polypropylene microtiter plate. Fractions collected in the region of interest (i.e. that where the mass spectrometer showed the presence of *m/z* 447, the protonated molecular ion of the glucuronide metabolite) were injected (5 µL) onto a second Polaris C18 column using the same mobile phase gradient to test for purity. Those containing the product of interest were combined into a 15 mL conical glass tube and the solvent was evaporated by vacuum centrifugation in the Genevac evaporator. Upon dryness they were prepared for NMR analysis as described below.

Example B: Activity-Gram and Biosynthesis of Two Hydroxy Metabolites of Compound B Using Method 1. Compound B (10 µM) was incubated with dog liver microsomes (2 mg/mL) in KH_2PO_4 (0.1M, pH 7.4) containing $MgCl_2$ (3.3 mM) and NADPH (1.3 mM) in a total volume of 1 mL at 37^o C. After 45 min, the incubation was terminated by addition of CH_3CN (5 mL), the precipitate was removed by centrifugation (5 min, 1700 x *g*), and the supernatant was evaporated in vacuo. The residue was reconstituted in 0.1 mL 1% formic acid and injected onto HPLC-MS. The system contained a Varian Polaris C18 column (4.6 x 250 mm; 5 µm) and a mobile phase

DMD Fast Forward. Published on July 22, 2014 as DOI: 10.1124/dmd.114.059204
This article has not been copyedited and formatted. The final version may differ from this version.

comprised of 0.1% formic acid (solvent A) and CH_3CN (solvent B) at a flow rate of 0.8 mL/min. The gradient program began with 95%A/5%B for 5 min followed by a linear gradient to 20%A/80%B at 50 min. The effluent was split between the mass spectrometer and a fraction collector at a ratio of about 1:15. The fractions were collected every 24 sec in a 96-well microtiter plate. The plate was transferred to a vacuum centrifuge to dry the plate. After drying, the plate was provided to the *in vitro* pharmacology laboratory (Pfizer. Groton, CT) and each well was tested for inhibition of phosphodiesterase-2 activity. By plotting the PDE2 activity observed in each well against the time of collection for each well, a chromatographic representation of pharmacological activity can be made. This representation has been called an activity-gram, (Obach, 2013). This activity-gram showed that the two hydroxyl metabolites could have PDE-2 inhibition activity, albeit the signal was weak. Nevertheless, observation of these signals in the activity-gram triggered a larger-scale biosynthesis of these two metabolites with the intent of more accurately evaluating their pharmacological activity on the isolated materials.

Compound B (20 µM) was incubated with dog liver microsomes (2 mg/mL) containing 3.3 mM $MgCl_2$, and 1.3 mM NADPH in a total volume of 50 mL KH_2PO_4 (100 mM, pH 7.4. The incubation was conducted in a 500 mL Erlenmeyer flask in a shaking water bath maintained at 37^o C for 1 hr. At the end of the incubation, 50 mL CH_3CN was added, the mixture was transferred to four 50 mL polypropylene conical tubes and vigorously mixed on a vortex mixer. The tubes were centrifuged at 1700 x *g* for 5 min and the supernatant was transferred to four new 50 mL polypropylene conical tubes. The tubes were subjected to vacuum centrifugation in a Genevac Evaporator (set at HPLC Mixture setting) for approximately 1 hr to remove the CH_3CN. To the remaining solution was added water to a total volume of ~100 mL and formic

acid (1 mL). This mixture was subjected to centrifugation at 40000 x *g* for 30 min to clarify the supernatant. The supernatant was transferred to a 100 mL graduated cylinder and directly applied onto a Varian Polaris C18 column (4.6 x 250 mm; 5 µm particle size) through a Jasco HPLC pump at a flow rate of 0.8 mL/min. Following application of the 100 mL, another ~10 mL of 0.1% formic acid was pumped onto the column to ensure that the HPLC lines were cleared of the supernatant.

The HPLC column was then transferred to the Thermo HPLC-MS system as in Example A. The effluent was split between the mass spectrometer and fraction collector at a ratio of approximately 1:15. The mobile phase composition and gradient was the same as used for the activity-gram described above. The mobile phase program and data collection was started by making a dummy injection of water from the autosampler. Fractions were collected every 20 sec into a wide-welled polypropylene microtiter plate. Fractions collected in the region of interest (i.e. that where the mass spectrometer showed the presence of *m/z* 390, the protonated molecular ion of hydroxy metabolites) were injected (5 µL) onto a second Polaris C18 column using the same mobile phase gradient to test for purity. Those containing the two products of interest were each combined into 15 mL conical glass tubes and the solvent was evaporated by vacuum centrifugation. The residues were prepared for NMR analysis as described below.

Example C: Biosynthesis of Compound C Hydroxy Metabolite Using Method 1. Compound C (40 µM) was incubated with human liver microsomes (1.0 mg/mL) containing 5 mM $MgCl_2$, and 1.3 mM NADPH in a total volume of 20 mL KH_2PO_4 (100 mM, pH 7.4). The incubation was conducted in a 200 mL Erlenmeyer flask in a shaking water bath maintained at 37^o C for 1.0 hr. At the end of the incubation, 80 mL CH_3CN was added; the mixture was transferred to three 50 mL polypropylene conical tubes and vigorously mixed on a vortex mixer. The tubes were spun

DMD Fast Forward. Published on July 22, 2014 as DOI: 10.1124/dmd.114.059204
This article has not been copyedited and formatted. The final version may differ from this version.

in a centrifuge at 1700 x *g* for 5 min and the supernatant was transferred to three new 50 mL polypropylene conical tubes. The tubes were subjected to vacuum centrifugation in a Genevac Evaporator (set at HPLC Mixture setting) for approximately 2 hr to remove the CH_3CN. The remaining solutions were combined and water was added to a total volume of ~100 mL and formic acid (1 mL). This mixture was subjected to centrifugation at 40000 x *g* for 30 min to clarify the supernatant. The supernatant was transferred to a 100 mL graduated cylinder and directly applied onto a Varian Polaris C18 column (4.6 x 250 mm; 5 µm particle size) through a Jasco HPLC pump at a flow rate of 0.8 mL/min. Following application of the 100 mL, another ~15 mL of 0.1% formic acid was pumped onto the column to ensure that the HPLC lines were cleared of the supernatant.

The HPLC column was then transferred to an HPLC-MS system as in Example A. The effluent was split between the mass spectrometer and a Gilson fraction collector at a ratio of approximately 1:15. The mobile phase used consisted of 0.1% formic acid (mobile phase A) and CH_3CN (mobile phase B) at a flow rate of 0.5 mL/min. The mobile phase composition commenced at 90%A/10%B, was held at that composition for 5 min, followed by a linear gradient to 5%A/95%B at 25 min, held at this composition for 5 min, then reequilibrated at initial conditions for 15 min. The mobile phase program and data collection was started by making a dummy injection of water from the autosampler. Fractions were collected every 20 sec into a wide-welled polypropylene microtiter plate. Fraction purity was assessed using a Halo C18 column (3.0 x 50 mm; 2.7 µm particle size) on an HPLC-MS system consisting of a Shimadzu CBM-20A controller, LC-20ADXR pumps, CTC PAL Autosampler and Agilent 1100 PDA in line with an AB Sciex Triple TOF 5600 mass spectrometer operated in the positive ion mode. The mobile phase used consisted of 0.1% formic acid (mobile phase A) and CH_3CN

DMD Fast Forward. Published on July 22, 2014 as DOI: 10.1124/dmd.114.059204
This article has not been copyedited and formatted. The final version may differ from this version.

(mobile phase B) at a flow rate of 0.45 mL/min. The mobile phase composition commenced at 95%A/5%B, was held at that composition for 1 min, followed by a linear gradient to 0%A/100%B at 7.9 min, held at this composition for 1 min, then reequilibrated at initial conditions for 2 min. Those fractions containing the product of interest were combined into 15 mL conical glass tubes and the solvent was evaporated by vacuum centrifugation. Upon dryness they were prepared for NMR analysis as described below.

Example D: Biosynthesis of Compound D Hydroxy Metabolite Using Method 2. The hydroxy metabolite of Compound D which had been detected in dog and human intestinal microsomal incubations was scaled up for isolation. Two separate incubations of Compound D were carried out in 50 mL polypropylene centrifuge tubes at 37° C for 40 minutes in a shaking water bath. The incubation volume was 10 mL and consisted of 0.1 M KH_2PO_4 buffer (pH 7.4), $MgCl_2$ (3.3 mM), dog intestinal microsomes (1.0 mg/mL), compound D (100 µM), and NADPH (1.3 mM). Reactions were terminated by the addition of CH_3CN (20 mL). The solutions were centrifuged (1800 x *g*, 5 minutes), and the supernatants were transferred to clean 50 mL polypropylene centrifuge tubes and concentrated to dryness. The residue in each tube was reconstituted with 600 µL of 10% CH_3CN in water. The reconstituted samples were combined in a 2 mL HPLC vial and were placed onto a Shimadzu semipreparative HPLC-UV system. The sample was injected as four 300 µL injections collecting the post column effluent on a fraction collector. Separation was performed on a Zorbax RX C8, 9.4 x 250 mm, 5 µm semi preparative HPLC column (Agilent). The mobile phase consisted of 0.1% formic acid (solvent A) and CH_3CN (solvent B) at a flow rate was 4.0 mL/min. The gradient started at 15% B for 5 min, ramped linearly to 90% B over 35 minutes, held isocratically at 90% B for 10 min, returned to the initial condition over 1.0 min, and allowed to equilibrate for 4.0 min. HPLC fractions were collected

DMD Fast Forward. Published on July 22, 2014 as DOI: 10.1124/dmd.114.059204
This article has not been copyedited and formatted. The final version may differ from this version.

throughout the run at 1.0 min intervals. Aliquots (100 µL) of fractions at the retention time of the ultraviolet peak corresponding to the hydroxy metabolite were analyzed by liquid chromatography-mass spectrometry. Fractions containing the metabolite of interest were combined into a single 15 mL glass centrifuge tube and concentrated to dryness. The residues were reconstituted in 200 µL DMSO-d_6 for NMR analysis.

Example E: Biosynthesis of Two Hydroxy Metabolites of Atazanavir Using Method 1.

Atazanavir (30 µM) was incubated with recombinant heterologously expressed CYP3A5 (58 pmol/mL) in 30 mL KH_2PO_4 (0.1 M, pH 7.4) containing $MgCl_2$ (3.3 mM) and an NADPH regeneration system (BD Gentest, Woburn, MA) at 37^o C in a shaking water bath. After 100 min, CH_3CN was added (30 mL) and the mixture was spun at 1700 x *g* for 5 min. The supernatant was transferred to 50 mL polypropylene conical tubes and subjected to vacuum centrifugation in a Genevac Evaporator (set at HPLC Mixture setting) for approximately 1 hr to remove the CH_3CN. To the remaining solution was added 0.5 mL formic acid and water to a total volume of 50 mL. This solution was spun at 40000 x *g* for 30 min, the resulting supernatant was transferred to a 50 mL graduated cylinder and directly applied onto a Varian Polaris C18 column (4.6 x 250 mm; 5 µm particle size) through a Jasco HPLC pump at a flow rate of 0.8 mL/min. Following application of the 50 mL, another ~10 mL of 0.1% formic acid was pumped onto the column to ensure that the HPLC lines were cleared of the supernatant. This column was transferred to the aforementioned HPLC-MS system (as in Example A). The products were eluted using a mobile phase gradient consisting of 0.1 % formic acid in water (solvent A) and CH_3CN (solvent B) at 0.8 mL/min. The mobile phase started at 5%B for 5 min, an instant increase to 25%B at 5.1 min, a linear gradient to 65%B at 50 min, a 10 min wash at 95%B and re-equilibration to initial conditions over 10 min. The eluent was passed through a photodiode

array UV detector (200-400 nm) and then split (approximately 1:6) between the LTQ mass spectrometer and a fraction collector. Fractions were collected every 20 sec. Each fraction collected in the retention time region of interest where hydroxyatazanavir metabolites eluted (~22-24 min) was tested for purity by HPLC. Those fractions containing products of interest were combined as appropriate into 15 mL conical glass tubes and the solvent removed in vacuo. This material was analyzed by NMR.

NMR Sample Preparation and Analysis. All samples, including parent compounds, were prepared for NMR analysis as follows. Tubes containing the dried products (isolates are typically not visible to the naked eye) were transferred to a vacuum chamber which was attached to a Vacuum Atmospheres Nexus II dry box. The samples were left under vacuum (-30 psi) for a minimum of one hour prior to entry to the glove box. The glove box was maintained at slightly positive pressure under 100% argon. All samples were dissolved in the highest available purity deuterated DMSO (typically "100%" grade DMSO-d6 which is 99.96 % deuterium enriched) using a minimum amount of solvent to achieve proper sample height in the NMR tube. This volume is 40 µL for samples prepared for 1.7 mm tubes and is 150 µL for samples prepared for 2.5 mm tubes. After addition of the solvent, samples were vortexed for 15 to 30 seconds, transferred to NMR tubes, capped and removed from the glove box. All transfer pipettes, pipette tips and NMR tubes were stored in the glove box to remove adsorbed water from their surfaces in order to minimize the potential for sample contamination.

NMR spectra were recorded on a Bruker Avance 600 MHz controlled by Topspin V3 and equipped with a 5 mm or 1.7 mm TCI Cryo probe. 1D spectra were recorded using an approximate sweep width of 8400 Hz and a total recycle time of ~7 s. The resulting time-averaged free induction decays were transformed using an exponential line broadening of 1.0 Hz

DMD Fast Forward. Published on July 22, 2014 as DOI: 10.1124/dmd.114.059204
This article has not been copyedited and formatted. The final version may differ from this version.

to enhance signal to noise. The 2D data were recorded using the standard pulse sequences provided by Bruker. At a minimum a 1K x 128 data matrix was acquired using a minimum of 2 scans and 16 dummy scans with a spectral width of 10000 Hz in the f2 dimension. The data was zero-filled to at least 1k data point. ^{1}H and ^{13}C spectra were referenced using residual DMSO-d_6 (^{1}H δ=2.50 relative to TMS, δ=0.00, ^{13}C δ=39.50 relative to TMS, δ=0.00).

qNMR was performed in three ways, using the aSICCO method (Walker, et al., 2011), the ERETIC2 (Bruker 2012) method or using an internal standard of maleic acid (Malz 2005). For aSICCO and ERETIC2 an authentic 10 mM standard of maleic acid was used as a calibrant.

DMD Fast Forward. Published on July 22, 2014 as DOI: 10.1124/dmd.114.059204
This article has not been copyedited and formatted. The final version may differ from this version.

RESULTS

Compound A. Compound A is a kyurenine aminotransferase inhibitor with a hydroxamic acid motif (Tuttle, et al., 2013). The *O*-glucuronide conjugate of compound A was successfully prepared from compound A incubated with human liver microsomes and conditions and cofactors to support glucuronidation reactions. In the HPLC trace of the isolation of compound A glucuronide (Figure 2, Panels A and B) it can be observed that two glucuronide metabolites were formed. Compound A can undergo glucuronidation at the hydroxamic acid oxygen and the amine nitrogen. The N-glucuronide was the minor product and not further characterized. The major glucuronide of interest was the O-glucuronide, eluting around 17.4 min. The fractions containing the *O*-glucuronide appeared pure by HPLC/UV-MS analysis (Figure 2, Panels C and D). NMR spectral data confirmed the overall purity of the sample and the site of glucuronidation as the hydroxamic acid oxygen. The structure was confirmed with three critical pieces of NMR data: (i) the presence of a ^{1}H resonance (δ 5.04, doublet, 1H, J=7.9 Hz) not observed in the parent; (ii) the ^{1}H-^{13}C HSQC data that linked this new ^{1}H resonance to a ^{13}C resonance at δ 109.6, and (iii) a positive NOE response in H7 when the new resonance at δ 5.04 is irradiated (Figure 3 Panels A, B and C). This data can only be satisfied by glucuronidation of the hydroxamic acid substituent. The concentration of the sample, determined by qNMR (aSICCO), was 0.053 mM.

This material was used as a standard for bioanalysis of in vivo matrices. *O*-Glucuronides arising from direct glucuonidation have the potential to undergo in-source fragmentation, and if not chromatographically resolved from their parent drugs, their presence can confound quantitation of the parent drug. This material was used to show that this phenomenon was not

operative in this case. The material was also used in a rat pharmacokinetic study to address the potential for enterohepatic recirculation. Rats showed high oral bioavailability and low clearance despite rat *in vitro* metabolism data demonstrating a high rate of glucuronidation. Analysis of bile from bile duct cannulated rats following intravenous and oral administration of compound A showed that the glucuronide was present at 26% (IV) and 39% (PO) of the dose in bile.

Compound B. In the example of the phosphodiesterase inhibitor compound B (Helal, et al., 2012), an observation had been made that the pharmacological effect observed in dogs was greater than what would be expected from the known potency of compound B and its concentration in plasma. Thus, the potential existed for an active metabolite(s). Compound B was incubated with dog liver microsomes and the metabolites observed (Figure 4 Panel A) included two hydroxyl metabolites (*m/z* 390), one doubly hydroxylated metabolite (*m/z* 406, retention time approximately 29 min), and two metabolites arising from oxidative opening of the azetidine ring (*m/z* 406, retention time = 18.77 min and *m/z* 392, retention time = 30.40 min). The fractions were tested for *in vitro* pharmacological activity to yield an activity-gram (Figure 4 Panel B). In addition to the unconsumed parent drug, there were two other peaks of activity that correlated with the two singly hydroxylated metabolites.

Upon observing that the two hydroxyl metabolites appeared to have some activity at the target enzyme, a larger scale biosynthesis was undertaken, using dog liver microsomes. The HPLC purification chromatogram is shown in Figure 5 (Panel A) and shows a complex array of metabolite peaks, of which two major peaks were the two metabolites of interest (shown in the XIC trace *m/z* 390 in Figure 5, Panel B). Analytical HPLC analysis of the individual samples indicated the isolates were pure, Figure5 (Panel C and D). The fractions containing the two

DMD Fast Forward. Published on July 22, 2014 as DOI: 10.1124/dmd.114.059204
This article has not been copyedited and formatted. The final version may differ from this version.

metabolites of interest were assessed by NMR and the sites of oxidation and the concentrations of metabolites B1 and B2 were determined (Figure 6). In the ^{1}H spectrum of compound B the resonance at δ 2.19 is assigned as the methylene C25 (Figure 6, Panel A) (for a complete numbering scheme of all compounds see supplemental data Figure 4). The ^{1}H of C24 and C26 were only observed as shallow broad peaks at δ 3.75. The absence of the ^{1}Hs of C24 and C26 is most likely due to ring inversions of the azetidine. This is important in the characterization of metabolite B1. The ^{1}H resonance of the methylene C25 observed in compound B was not observed in the ^{1}H spectrum of metabolite B1, nor were the ^{1}H resonances of C24 and C26 (Figure 6, Panel C). However, all other ^{1}H resonances in the metabolite B1 spectrum were present and unmodified from those observed in the parent compound. Because of this the exact site of oxidation for metabolite B1 could only be implied as on C24, C25 or C26. However, if the site of oxidation was on either the C24 or C26 the resulting metabolite would be a carbanolamine and would likely be unstable. Because the metabolite appeared to be sufficiently stable to isolate, the oxidation is assigned to the C25 carbon. The ambiguity in the structural assignment had no impact on the determination of concentration of the metabolite B1. There was an abundance of resonances in which the number of hydrogens were known thus allowing the concentration calculation. The concentration of metabolite B1 was determined to be 0.048 mM (aSICCO).

The chemical structure of metabolite B2 was definitively identified based on ^{1}H NMR data. Compound B contains a pendent ethyl group on the phenyl ring. In the ^{1}H NMR spectrum of the parent compound the methyl of the pendent ethyl is assigned as a triplet at δ 1.15 (3H, J= 7.5 Hz) and the methylene is assigned as a quartet at δ 2.58 (2H, J= 7.5 Hz). In a similarly acquired spectra of the isolated metabolite B2 these resonances have changed (Figure 6, Panel

B). The methyl resonance is now a doublet at δ 1.28 (3H, *J*= 6.5 Hz) and the methylene has changed to a methine and is assigned to the quartet at δ 4.67 (1H, *J*= 6.5 Hz). The concentration of metabolite B2 was 0.92 mM (aSICCO). These stock solutions were then used to determine the target enzyme IC_{50} of the metabolites at 10 nM and 42 nM (for B1 and B2, respectively), as compared to 2 nM for the parent compound B. These metabolites were observed in dog plasma at greater concentrations than compound B itself, and thus the disparity in the concentration-effect relationship in dog could be rationalized.

Compound C. The hydroxyl metabolite of compound C was successfully prepared from incubations of compound C with human liver microsomes and conditions and cofactors to support P450 oxidation. In the HPLC trace of the isolation of metabolite C1 (Figure 7 Panel A) it can be observed that one major metabolite was formed, retention time 24.32 min. CID spectra of compound C and metabolite C1 indicate the presence of a single hydroxylation on one of the tert-butyl groups. The fractions containing the hydroxyl metabolite were pure (Figure 7, Panel B), and a stock concentration in DMSO-d_6 was 8.2 mM as determined by qNMR (ERETIC2). The definitive NMR data that enables the structural assignment of metabolite C1 was the ^{1}H and ^{1}H-^{13}C HMBC data sets (Figure 8). The 1D ^{1}H data of the isolated metabolite C1 contains two singlet peaks at δ 1.30 and δ 1.39 integrating to six and nine hydrogens, respectively. Additionally there is a new singlet resonance not observed in the parent compound at δ 3.65 integrating as two hydrogens. These data are consistent with the oxidation of one of the two t-butyl groups found on compound C. However, this cannot delineate which t-butyl moiety was oxidized. In order to identify the site of oxidation, HMBC data must be used (Figure 8). In the HMBC data set of metabolite C1 the t-butyl resonance (δ 1.39) correlates to a quaternary carbon atom with a chemical shift of δ 132.4, Figure 8 Panel B. The resonance at δ 11.81 (assigned as

the amide NH) also has a correlation to the same carbon at δ 132.4, Figure 8 Panel A. The only way to resolve these data is to assign the oxidation to the t-butyl para to the amide of compound C. This material was used as a substrate for blood-to-plasma ratio determination (compound C = 0.780, metabolite C1 = 0.615), human plasma protein binding (fraction unbound, compound C = 0.00013, metabolite C1 = 0.0028), and *in vitro* efficacy determinations (EC_{50} compound C = 7 nM and metabolite C1= 19 nM) to aid understanding the contribution of metabolite C1 to preclinical in vivo efficacy models.

Compound D. Compound D is a microsomal triglyceride transfer protein (MTP) inhibitor which contains a metabolically labile ester linkage (Ryder et al., 2012). The primary metabolite of compound D was prepared from an incubation of Compound D with dog intestinal microsomes. The HPLC analysis of the final incubate revealed a single dominant metabolite, metabolite D1, eluting prior to compound D, Figure 9 Panel A. Semi-preparative HPLC isolation of this metabolite yielded a chromatographically pure isolate containing a single peak, Figure 9 Panel B. HPLC-MS data indicated metabolite D1 to have a mass of *m/z* 691, 16 Da greater than compound D, indicating a single site oxidation. MS/MS data demonstrated the oxidation was on the isobenzofuranone portion of the molecule. The NMR analysis indicated the isolated metabolite was mixture of two diastereomers resulting from the oxidation of C2 in the isobenzofuranone. The critical NMR data that determined the site of oxidation are the ^{1}H-^{13}C HSQC data sets for compound D and metabolite D1, Figure 10. In the ^{1}H-^{13}C HSQC data of compound D the cross peak at ^{1}H 5.08/^{13}C 73.3 is assigned as C2 of the benzofuran, Figure 10, Panel A (for a complete numbering scheme of all compounds see supplemental data Figure 4). In a similarly acquired data set of the isolated metabolite these resonances are absent and two new ^{1}H resonances appear at δ 6.37 and δ 6.48. In the multiplicity edited ^{1}H-^{13}C HSQC these

DMD Fast Forward. Published on July 22, 2014 as DOI: 10.1124/dmd.114.059204
This article has not been copyedited and formatted. The final version may differ from this version.

resonances are correlated to a ^{13}C chemical shift of δ 101.4 and indicate both arise from methines (Figure 10, Panel B). This is consistent with the isolate being a mixture of diastereomeric alcohols resulting from oxidation of the C2 carbon of compound D. Using an internal standard of 10 mM maleic acid the concentration of the sum of both diastereomers together was determined to be 0.18 mM. The isolated metabolite was also used as substrate to determine its gMTP inhibitory IC_{50} value and was shown to be 30 fold less active than Compound D and is therefore no concern.

Atazanavir. Two hydroxyatazanavir metabolites were prepared from an incubation of atazanavir and human CYP3A5. In the HPLC trace of the incubation extract (Figure 11, Panel A) there are two very closely eluting metabolites of *m/z* 720 (Figure 11, Panel B). The earlier eluting metabolite was present in a fraction that contained a contamination of the later eluting metabolite (Figure 11, Panel C) while the later eluting metabolite had only a trace of the earlier metabolite (Figure 11, Panel D).

The ^{1}H spectrum of atazanavir contains ^{1}H resonances at δ 7.42 and δ 7.97 that are both doublets with coupling constants of 8.2 Hz each integrating to two ^{1}H (Figure 12, Panel A). The COSY data set indicates these resonances are strongly coupled to each other and to no other protons. These resonances are easily assignable to the four resonances of the single para substituted ring in atazanavir; H8, H9, H11 and H12 (for a complete numbering scheme of all compounds see supplemental data Figure 4). In the ^{1}H spectrum of metabolite E1 the resonances of H8, H9, H11 and H12 are also present and unmodified from those observed in atazanavir. The resonances for H35, H36, H37, H38 and H39 are either absent or significantly shifted. Additionally, there is a new set of resonances that are consistent with a para substituted phenyl ring at δ 6.58 and δ 6.95 that are both doublets with coupling constants of 7.9 Hz and each integrate to two protons

DMD Fast Forward. Published on July 22, 2014 as DOI: 10.1124/dmd.114.059204
This article has not been copyedited and formatted. The final version may differ from this version.

(Figure 12, Panel B). The COSY data of the isolate of metabolite E1 also indicates these resonances are strongly coupled to each other and no to other protons. The resonances are most easily explained by the oxidation of C37 to form a para substituted phenol. Using qNMR (ERETIC 2), the concentration of the E1 metabolite was determined to be 0.05 mM and contained approximately 30% contamination of the E2 metabolite.

In the ^{1}H spectrum of atazanavir the resonances δ 0.63 and δ 0.77 (each singlets integrating to 9 Hs) are assigned as the t-butyl groups (Figure 12, Panel C). Because of the size and near symmetry of atazanavir these two groups cannot be readily distinguished by NMR. In the ^{1}H spectrum of the metabolite E2, the resonance at δ 0.63 has neither changed in chemical shift nor in integration. However, the δ 0.77 resonance has shifted slightly to δ 0.70 and now appears as a two singlets of equal intensity, with an integration equaling six protons. Additionally observed in the ^{1}H spectrum of the isolate are two new resonances at δ 3.03 and δ 3.14, Figure 12, Panel D. The multiplicity edited ^{1}H-^{13}C HSQC data set indicates these resonances are inequivalent methylenes with a correlation to a carbon resonance at δ 67.5, while the δ 0.63 and δ 0.77 are methyls or methines correlating to carbon resonances at δ 26.2 and δ 21.3 respectively. Based on the ^{1}H and ^{13}C chemical shifts the resonances at δ 0.70 are assigned as a pair of methyl groups with two separate chemical shifts. All of the NMR data from the E2 metabolite strongly suggests an oxidation of one of the t-butyl groups. In order to define which t-butyl has been oxidized MS/MS data was necessary. Atazanavir and the isolated metabolite E2 were analyzed on an Orbitrap mass spectrometer to develop a fragmentation pattern (supplemental Figures 1-3). Among the array of mass spectral fragments, metabolite E2 yielded a very minor ion at *m/z* 351.1915 indicating that the hydroxylation was on the portion indicated by carbons 18-51 (see supplemental data Figure 4) and this fragmented further to *m/z* 164.1065 (unmodified 1-hydroxy-

2-amino-4-phenylbutane). These were the only fragment ions that yielded the information needed to show which of the two t-butyl groups was hydroxylated in metabolite E2. Using qNMR, the concentration of the E2 metabolite was determined to be 0.60 mM (ERETIC 2).

These two materials were used in the construction of standard curves for an HPLC-MS assay that was used to measure the enzyme kinetics of atazanavir metabolism in human liver microsomes, CYP3A4, and CYP3A5 (Tseng, et al., 2014). This example demonstrates that in some cases metabolites do not even have to be pure for them to be of use.

DMD Fast Forward. Published on July 22, 2014 as DOI: 10.1124/dmd.114.059204
This article has not been copyedited and formatted. The final version may differ from this version.

DISCUSSION

In this report, we have described methods useful for the generation of standards of metabolites via biosynthesis and qNMR. Metabolite standards generated in this fashion can be used for determination of *in vitro* pharmacological activity, for the creation of standard curves needed for HPLC-MS bioanalysis and for vitro drug metabolism studies. Both oxidized and conjugated metabolites have been able to be generated and used in these types of experiments.

In general, the focus is on the generation of metabolites of relevance to humans and ideally a human *in vitro* system would ensure the production of the metabolite of interest including the relevant stereochemistry. However, in selecting a biological system for metabolite generation, it is best to select the system that will offer the greatest conversion to the metabolite of interest. In many instances, the best system to select may be liver microsomes from laboratory animal species and not human. Also, employment of heterologously expressed human enzymes for the biosynthesis of a metabolite can offer advantages. Others have demonstrated the usefulness of microbes or mutated cytochrome P450 enzymes (Li, et al., 2009). When using an alternate system, it is critical to ascertain that the metabolite generated matches the desired product (in regio- and stereochemistry). In each example described in this report, a preliminary investigation of various in vitro systems was done to identify the system that would yield the metabolite(s) of interest in the best yield and with anticipated ease of isolation.

In our experiences generating metabolites in this manner, we have observed some subtle, but critical technical aspects: (1) When loading an HPLC column by pumping a large volume of dilute aqueous extract through an HPLC pump, it is critical that the solution be clear and devoid of particles. Thus, spinning the solution at 40000 x *g* is an essential step, and monitoring the column back pressure is recommended. Organic modifier concentration must be low enough to

DMD Fast Forward. Published on July 22, 2014 as DOI: 10.1124/dmd.114.059204
This article has not been copyedited and formatted. The final version may differ from this version.

permit "packing" of the metabolite on the head of the column. (2) Upon obtaining an HPLC eluent fraction that possesses the metabolite of interest, we have found that removing the solvent in a vacuum centrifuge is superior to evaporation under inert gas. The material concentrates into the bottom of the tube for easier recovery into minimal (e.g. <0.05 mL) NMR solvent. We use conical glass tubes for this step. Drying under a flow of inert gas tends to spread the material over a larger surface area of the tube which can lead to higher losses during reconstitution and introduction of possible contaminants from the drying gas and lines. (3) The volume of HPLC solvent in which the isolate is collected should be minimized. HPLC solvents are not 100% pure thus the smaller the volume used in the collection the lower the concentration of the non-drug related impurities in the final isolate. (4) In almost all cases the two largest impurities in the ^{1}H NMR spectrum of an isolated metabolite are the residual non-deuterated solvent peak and water. The former can only be minimized through using the highest purity solvents available. Deuterated solvent manufacturers offer several levels of deuteration; obviously the more isotopically pure the solvent the greater the cost. However, when considering the total cost of the sample preparation (medicinal chemist time to synthesize the parent, the cost of hepatocytes/microsomes, the cost of isolation time etc.) the relative cost of the highest quality deuterated solvent is minimal. The minimization of water as a contaminant in NMR samples is also controllable. After removing solvent from the final isolate, the sample is transferred and prepared in a dry box so that the residual water in the sample will be minimal.

Once the highest quality sample is prepared the acquisition of the NMR data becomes the critical step in the process. NMR analysis is inherently less sensitive than MS analysis. However, since the introduction of reduced temperature probes (Bruker cryo probes, Varian cold probes) in the late 1990s the sample mass requirements for NMR have been consistently

DMD Fast Forward. Published on July 22, 2014 as DOI: 10.1124/dmd.114.059204
This article has not been copyedited and formatted. The final version may differ from this version.

dropping. The reduction of temperature in the acquisition coils of an NMR probe can increase the signal to noise (S/N) as much as a factor of four in a single pulse experiment over comparable room temperature probes. In multi-pulse experiments this results in a practical increase in S/N of approximately a factor of ten. Concomitant with the development of cryo probes was an effort to reduce the probe diameter and hence decrease the overall volume requirements for a sample. In terms directly relatable to a drug metabolism scientist, if 20 nmol of a metabolite is isolated and reconstituted in a volume for a 5 mm probe (0.6 mL) the resulting sample concentration is 0.03 mM. This same quantity reconstituted for a 1.7 mm probe (0.040 mL) will result in a final concentration of ~0.5 mM. It has been our experience that isolated samples with concentrations of 1.0 mM are usually sufficient for structural characterization and quantitation. Obviously this value is dependent on the complexity of the molecule. Sometimes other more sample-intensive experiments, direct observed carbon or ^{1}H-^{15}N HMBC for example, may be required. Conversely much less sample may be required if the molecular modification is on a spectroscopically isolated portion of a molecule.

As an alternative to using ^{1}H as the nuclei for quantitation, ^{19}F could also be used. ^{19}F qNMR has two distinct advantages over ^{1}H qNMR. First, the inherent background of contaminating resonances from the isolation process is negligible with ^{19}F NMR and secondly the spectral width of ^{19}F NMR is much larger that of ^{1}H (250 ppm for ^{19}F vs 12 ppm for ^{1}H) allowing much greater selectivity. However, there is the obvious disadvantage that the molecule of interest must contain a ^{19}F atom.

The examples described in this paper illustrate some uses of the biosynthesized metabolite solutions of known concentration in drug research. Metabolite stock solutions

generated using these methods can frequently range between 0.05 and 5 mM. In most cases, these concentrations are high enough to permit use of these solutions as parent stock solutions that can be diluted to make standard curves for HPLC-MS bioanalytical methods. The glucuronide of compound A was used to quantitate rat bile samples by HPLC-MS, in order to determine the fraction of compound A excreted as its glucuronide. Stock solutions of metabolites B1 and B2 were used to test target potency and to make standard curves for the determination of metabolite concentrations in dog plasma samples by HPLC-MS. These plasma exposure values were important for understanding the concentration-effect relationship. The isolated metabolite C1 was used to establish ADME parameters (blood-to-plasma ratio and human plasma protein binding) as well as potency, all of which helped to provide a better understanding of the efficacy of compound C. The stock solution of compound D was used in potency assays to help establish SAR around this chemical series. The hydroxyatazanavir metabolites were used as standards for making enzyme kinetic measurements for CYP3A4 and 3A5 catalyzed metabolism and aided in understanding the relative importance of these two enzymes in atazanavir metabolism in human (Tseng, et al., 2014).

Other uses of the solutions of biosynthesized metabolites included measurement of target receptor affinity. In the example of compound B, the activity-gram approach was used first to show that metabolites B1 and B2 could potentially have pharmacological activity, while the other metabolites would not. This triggered the biosynthesis and isolation of metabolites B1 and B2 and preparation of stock solutions of known concentration by qNMR which were diluted into assay buffer for determination of intrinsic potency. Ultimately, if a metabolite is deemed to be important for the activity of a new drug (either efficacy and/or safety), a large quantity (i.e. grams) will need to be prepared for in-depth study. The methods described in this work can be

used up-front to determine whether such an investment in synthesis is warranted. Or if synthesis of the metabolite is intractable, then biosynthesis and use of stock solutions of concentration established with qNMR may be the only avenue to have material for other investigations.

In conclusion, techniques to generate drug metabolites in stock solutions of known concentration have been described in detail. qNMR is critical to this procedure and the close collaboration between the drug metabolism scientist and NMR spectroscopist is essential. This is even more effective if the NMR instrumentation is established in the drug metabolism lab, since the needs for this technique differ from the use of NMR in medicinal and process chemistry. These techniques can be essential for gathering important information on the activity of metabolites, quantitative exposure to metabolites, and ADME properties of metabolites.

Authorship Contributions

Participated in research design – Walker, Ryder, Bauman, Obach and Smith

Conducted experiments – Walker, Ryder, Bauman and Obach

Performed data analysis –Walker, Ryder, Bauman and Obach

Wrote or contributed to the writing of the manuscript – Walker, Ryder, Bauman, Obach, Smith and Spracklin

REFERENCES

Baillie TA, Cayen MN, Fouda H, Gerson RJ, Green JD, Grossman SJ, Klunk LJ, LeBlanc B, Perkins DG, Shipley LA. (2002) Drug metabolites in safety testing. *Toxicol. Appl. Pharmacol.* 182: 188-196.

Bernadou J and Meunier B (2004) Biomimetic chemical catalysts in the oxidative activation of drugs. *Adv. Syn. Catal.* 346: 171-184.

Bruker Manual, (2012) ERETIC 2 User's Guide preliminary guide

Espina R, Yu L, Wang J, Tong Z, Vashishtha S, Talaat R, Scatina J, and Mutlib AE, (2009) Nuclear Magnetic Resonance Spectroscopy as a Quantitative Tool To Determine the Concentrations of Biologically Produced Metabolites: Implications in Metabolites in Safety Testing. *Chem. Res. Tox.* 22(2): 299-310

Helal CJ, Chappie TA, and Humphrey JM. (2012) Preparation of pyrazolopyrimidine derivatives for use as PDE2 and/or CYP3A4 inhibitors. PCT Int. Appl. WO 2012168817 A1 20121213.

ICH (2009) Guidance on nonclinical safety studies for the conduct of human clinical trials and marketing authorization for pharmaceuticals. M3(R2).

http://www.ich.org/fileadmin/Public_Web_Site/ICH_Products/Guidelines/Multidisciplinary/M3_R2/Step4/M3_R2__Guideline.pdf (Accessed December 22, 2013)

Li W, Rozzell D, Kambourakis S, and Mayhew M (2009) Biosynthesis of drug metabolites. In: Biocatalysis for the Pharmaceutical Industry: Discovery, Development, and Manufacturing (Ed: J Tao) Wiley pp 183-211.

Malz, F, Jancke, H, (2005) Validation of quantitative NMR. J. Pharm. Biomed. Anal. 38: 813–823

Obach RS (2013) Pharmacologically active drug metabolites: impact on drug discovery and pharmacotherapy. *Pharmacol. Rev.* 65: 578-640.

Parkinson A, Oglivie BW, Buckley DB, Kazmi F, Czerwinski M, and Parkinson O (2013) Biotransformation of xenobiotics. In: Casarett and Doull's Toxicology: The Basic Science of Poisons, 8th Edition (Ed. C. Klaassen), McGraw-Hill, New York, pp.185-366.

Pauli GF, Gödecke T, Jaki BU, Lankin DC (2012) Quantitative 1H NMR. Development and Potential of an Analytical Method: An Update J. Nat. Prod. 75(4): 834-851

Ryder T, Walker GS, Goosen TC, Ruggeri RB, Conn EL, Rocke BN, Lapham K, Steppan CM, Hepworth D, Kalgutkar AS, (2012) Insights into the Novel Hydrolytic Mechanism of a Diethyl

2-Phenyl-2-(2-arylacetoxy)methyl Malonate Ester-Based Microsomal Triglyceride Transfer Protein (MTP) Inhibitor", *Chem. Res. Tox.* 25(10): 2138-2152

Smith DA and Obach RS (2009)Metabolites in Safety Testing (MIST): Considerations of Mechanisms of Toxicity with Dose, Abundance, and Duration of Treatment. *Chem. Res. Toxicol.* 22: 267-279.

Tseng E, Walsky RW, Luzetti RA, Harris JJ, Kosa RE, Goosen TC, Zientek MA, and Obach RS (2014) Relative contributions of CYP3A4 vs. CYP3A5 for CYP3A cleared drugs assessed *in vitro* using a CYP3A4 selective inactivator (CYP3cide). Drug Metab. Dispos. 42(7): 1163-1173

Tuttle JB, Anderson M, Bechle BM, Campbell BM, Chang C, Dounay AB, Evrard E, Fonseca KR, Gan X, Ghosh S, Horner W, James LC, Kim JY, McAllister LA, Pandit J, Parikh VD, Rago BJ, Salafia MA, Strick CA, Zawadzke LE, and Verhoest PR (2013) Structure-Based Design of Irreversible Human KAT II Inhibitors: Discovery of New Potency-Enhancing Interactions. *ACS Med. Chem. Lett.* 4: 37-40

Vishwanathan K, Babalola K, Wang J, Espina R, Yu L, Adedoyin A, Talaat R, Mutlib A, and Scatina J (2009) Obtaining Exposures of Metabolites in Preclinical Species through Plasma Pooling and Quantitative NMR: Addressing Metabolites in Safety Testing (MIST) Guidance without Using Radiolabeled Compounds and Chemically Synthesized Metabolite Standards. *Chem. Res. Tox.* 22(2): 311-322

Walker GS, Ryder R, Sharma R, Smith EB, Freund A, (2011) Validation of Isolated Metabolites from Drug Metabolism Studies as Analytical Standards by Quantitative NMR. *Drug Metab. Dispos.* 39(3): 433-440

Zhang H, Davis CD, Sinz MW, and Rodrigues AD (2007) Cytochrome P450 reaction-phenotyping: an industrial perspective. *Exp. Opin. Drug Metab. Toxicol.* 3: 667-687.

DMD Fast Forward. Published on July 22, 2014 as DOI: 10.1124/dmd.114.059204
This article has not been copyedited and formatted. The final version may differ from this version.

FIGURE LEGENDS.

Figure 1. Example compounds and their metabolites of interest.

Figure 2. Preparation of Compound A Glucuronide. Panel A: HPLC Photodiode Array trace (200-400 nm) of the compound A glucuronide biosynthesis mixture applied to a Polaris C18 HPLC column. Panel B: Concurrent extracted ion chromatogram of *m/z* 447 indicating the elution time of the product of interest (~17.4 min). Panel C: HPLC-PDA (200-400 nm) trace of the fraction containing compound A glucuronide product (R_t = 18.2 min). Panel D: Concurrent XIC of *m/z* 447 of the fraction containing compound A.

Figure 3. NMR of Compound A Glucuronide. Panel A: ^{1}H-^{13}C HSQC , Panel B: ^{1}H, Panel C: 1D NOE excitation frequency at δ5.03 (H1')

Figure 4. HPLC-MS and Activity-Gram for Compound B in Dog Liver Microsomes. Panel A is the corresponding sum mass spectral trace for the ion currents of interest. Panel B is the inhibition of PDE2 measured in each fraction. Peaks possessing pharmacological activity were observed at retention times corresponding to two hydroxylated metabolites (~21 and ~25 min) and the parent compound (~29 min).

Figure 5. Preparation of Metabolites B1 and B2. Panel A: HPLC PDA trace (200-400 nm) of the compound B biosynthesis mixture applied to a Polaris C18 HPLC column. Panel B: Concurrent XIC of *m/z* 390 indicating the elution time of the products of interest (~21 and 25 min). Panels C and D: HPLC-PDA (200-400 nm) traces of the fractions containing metabolites B1 and B2.

DMD Fast Forward. Published on July 22, 2014 as DOI: 10.1124/dmd.114.059204
This article has not been copyedited and formatted. The final version may differ from this version.

Figure 6. NMR of compound B and its metabolites B1 and B2 Panel A: Aliphatic portion of the ^{1}H spectrum of compound B, Panel B: Aliphatic portion of the ^{1}H spectrum of compound B2, Panel C: Aliphatic portion of the ^{1}H spectrum of compound B1(for a complete numbering scheme of all compounds see supplemental data Figure 4).

Figure 7. Preparation of Metabolite C. Panel A: HPLC PDA trace (310-315 nm) of the compound C biosynthetic mixture applied to a Polaris C18 HPLC column. Panel B: Concurrent XIC of *m/z* 409 of the isolated fraction containing metabolite C1 applied to a Halo C18 HPLC column.

Figure 8. NMR of compound C1, Panel A ^{1}H-^{13}C HMBC (amide region), Panel B ^{1}H-^{13}C HMBC (methyl region).

Figure 9. Preparation of Metabolite D. Panel A: HPLC PDA trace (200-400 nm) of the compound D biosynthesis mixture applied to a Zorbax RX C8 (9.4 x 250 mm) HPLC column. Panel B: Extracted ion chromatogram of m/z 690 indicating the elution time of the product of interest (~31min) under analytical HPLC conditions.

Figure 10. NMR of compound D and its metabolite D1, Panel A ^{1}H-^{13}C HSQC of Compound D, Panel B ^{1}H-^{13}C HSQC of Compound D1 (for a complete numbering scheme of all compounds see supplemental data Figure 4).

DMD Fast Forward. Published on July 22, 2014 as DOI: 10.1124/dmd.114.059204
This article has not been copyedited and formatted. The final version may differ from this version.

Figure 11. Purification of Atazanavir metabolite

Purification of Atazanavir metabolites. Panel A: HPLC PDA trace (200-400 nm) of the Atazanavir biosynthesis mixture applied to a Polaris C18 HPLC column. Panel B: Concurrent XIC of *m/z* 720 indicating the elution time of the products of interest (~23 min). Panels C and D: HPLC-PDA (200-400 nm) traces of the fractions containing metabolites E1 and E2.

Figure 12. NMR data for atazanavir and its metabolites E1 and E2. Panel A: Aromatic portion of the ^{1}H spectrum of atazanavir , Panel B: Aromatic portion of the ^{1}H spectrum of compound E1, Panel C: Aliphatic portion of the ^{1}H spectrum of atazanavir and Panel D: Aliphatic portion of the ^{1}H spectrum of compound E2 (for a complete numbering scheme of all compounds see supplemental data Figure 4).

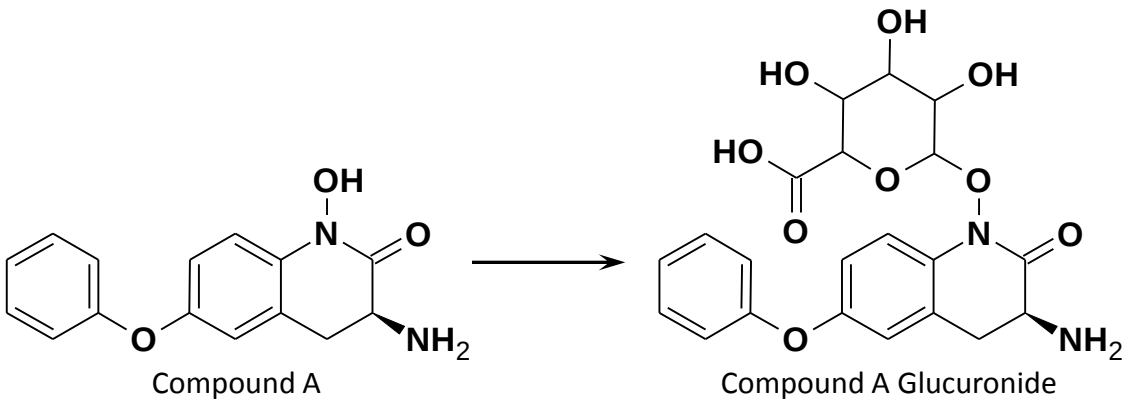

Compound A

Compound A Glucuronide

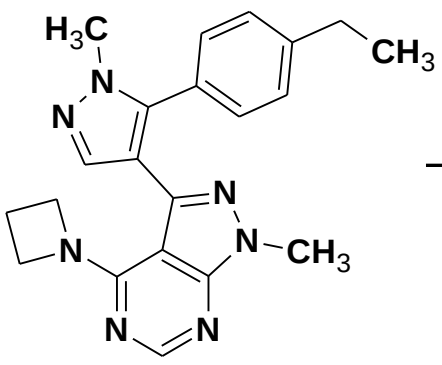

Compound B

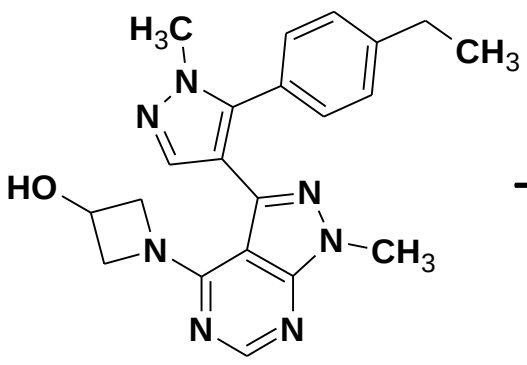

Metabolite B1

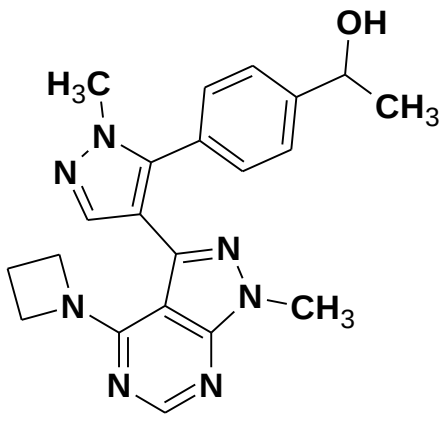

Metabolite B2

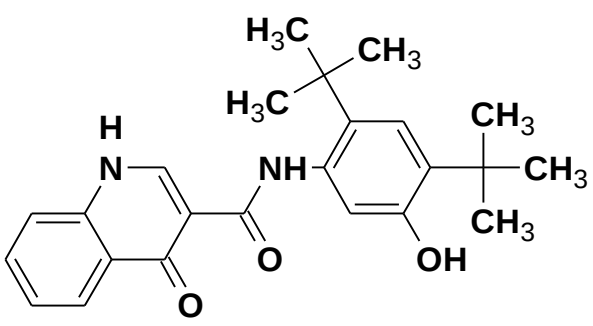

Compound C

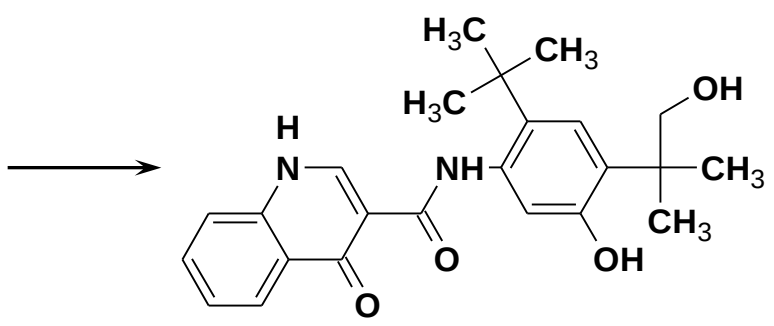

Metabolite C1

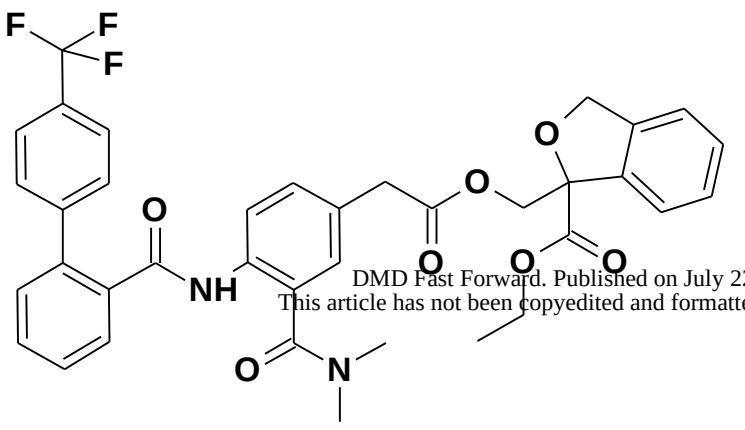

Compound D

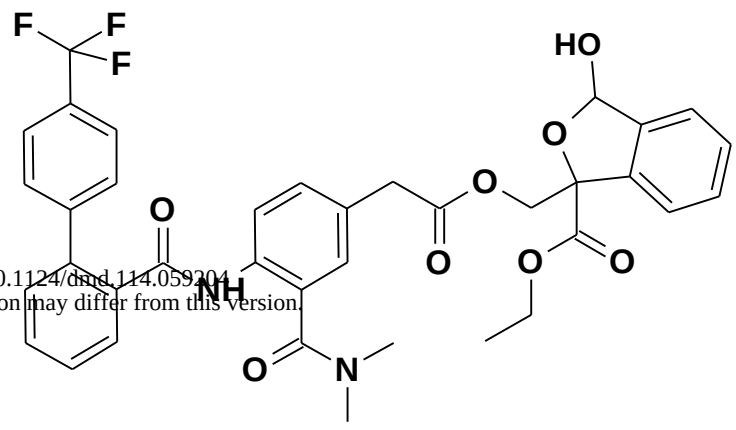

Metabolite D1

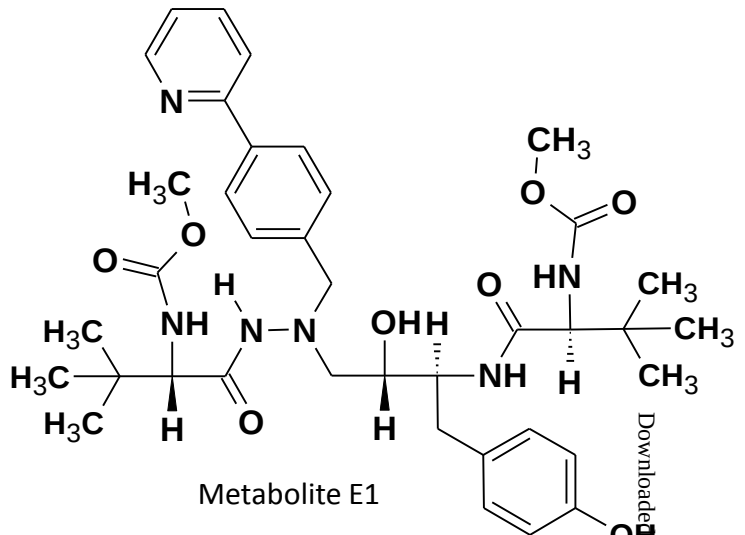

Metabolite E1

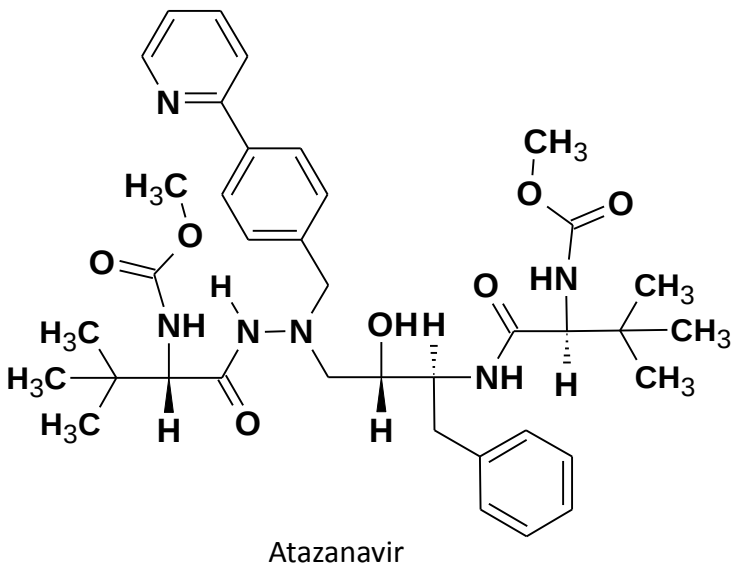

Atazanavir

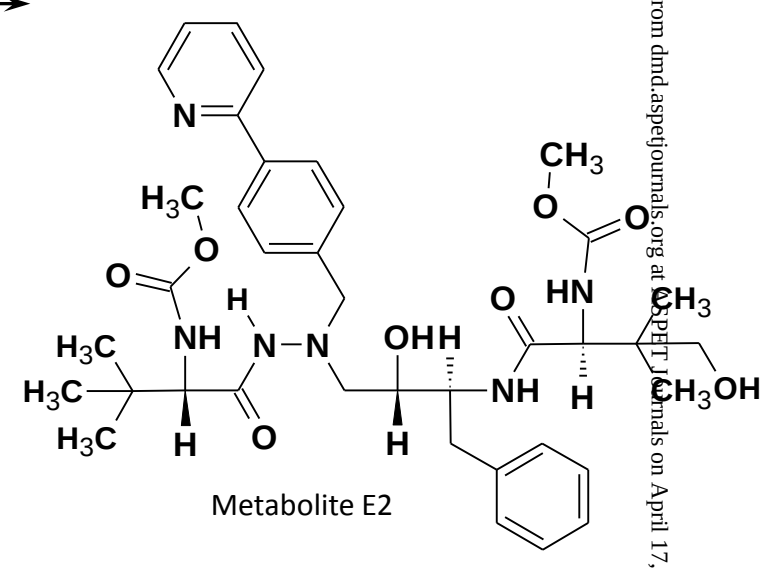

Metabolite E2

Figure 1

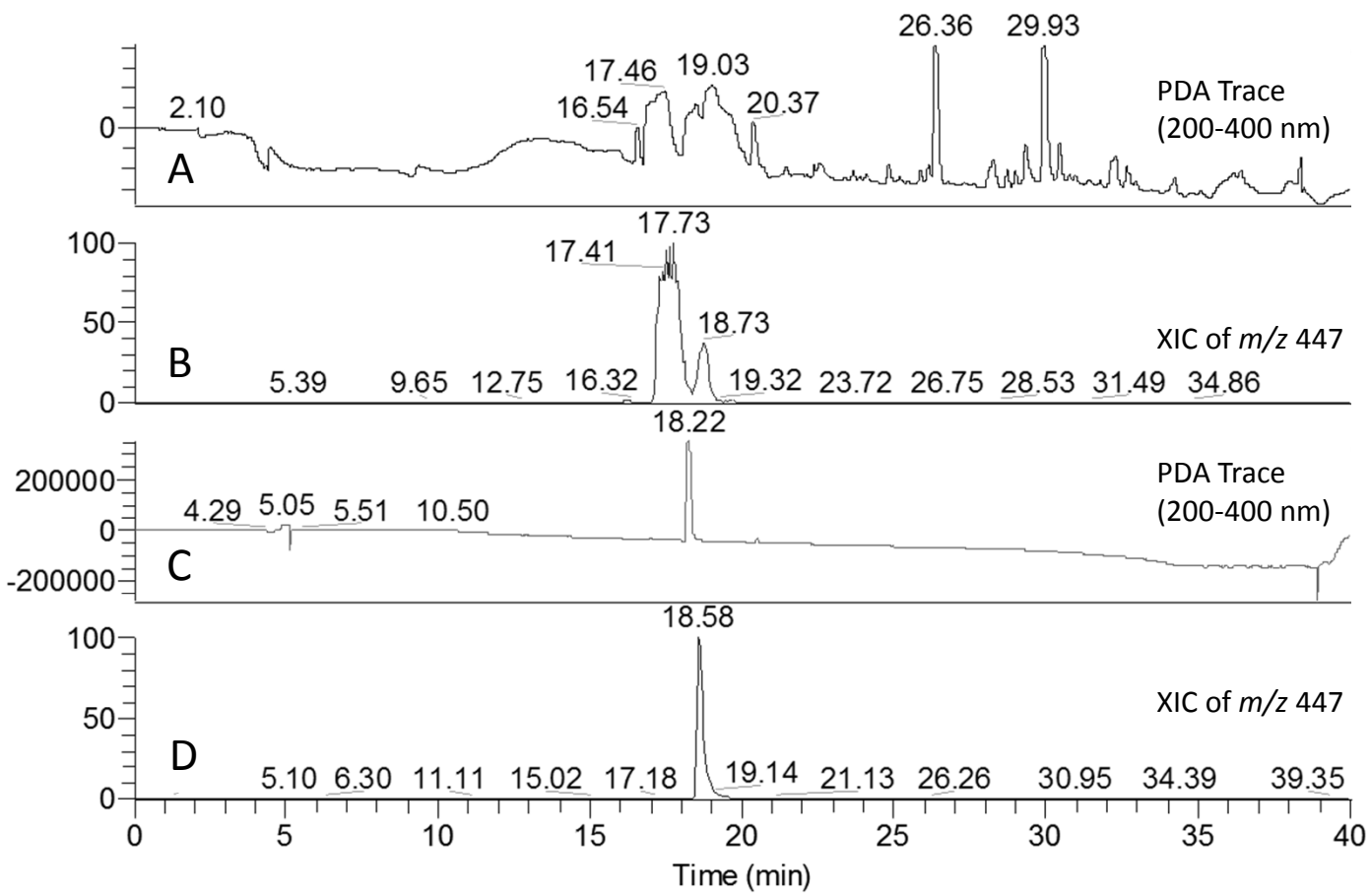

Figure 2

DMD Fast Forward. Published on July 22, 2014 as DOI: 10.1124/dmd.114.059204
This article has not been copyedited and formatted. The final version may differ from this version.

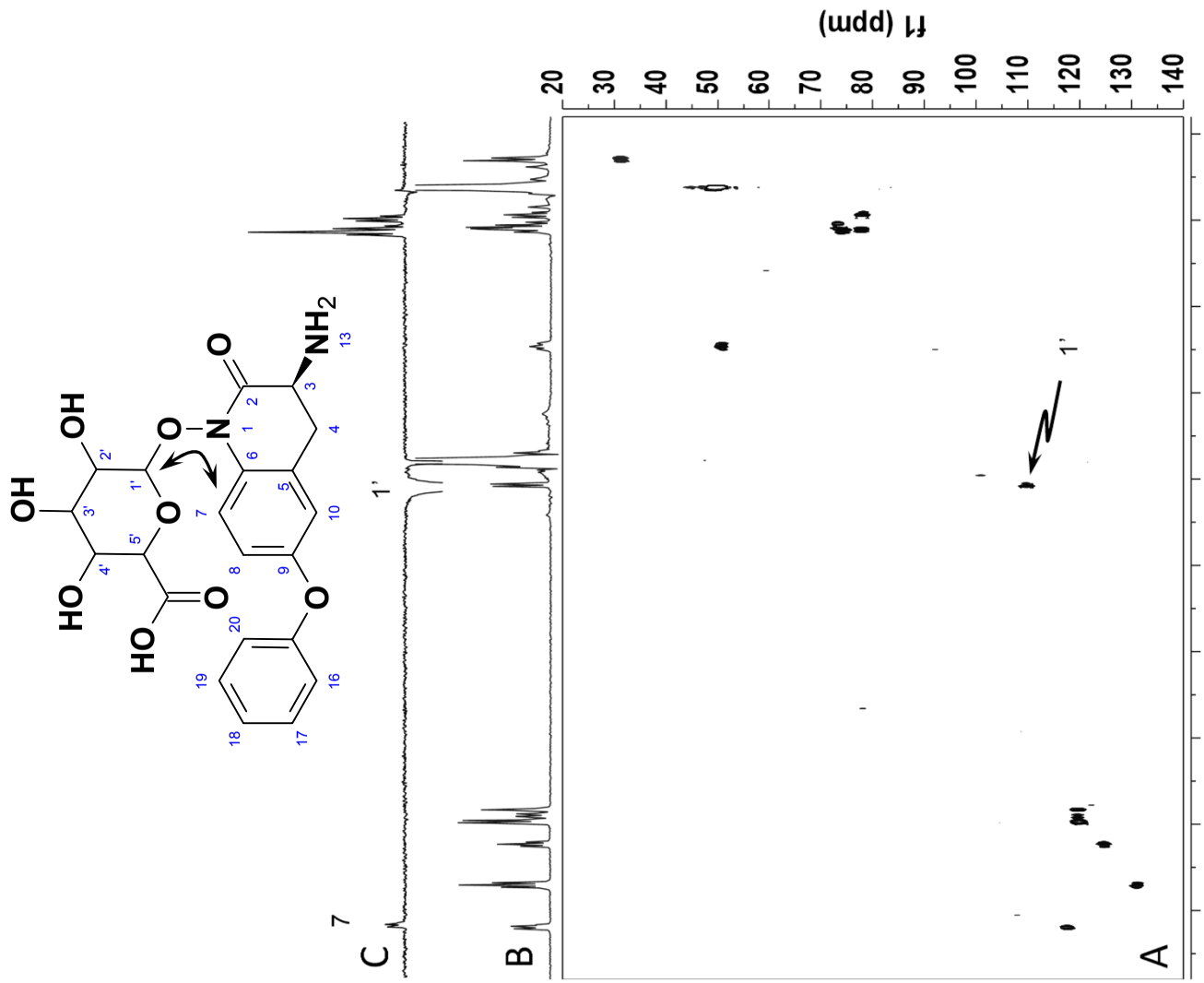

Figure 3

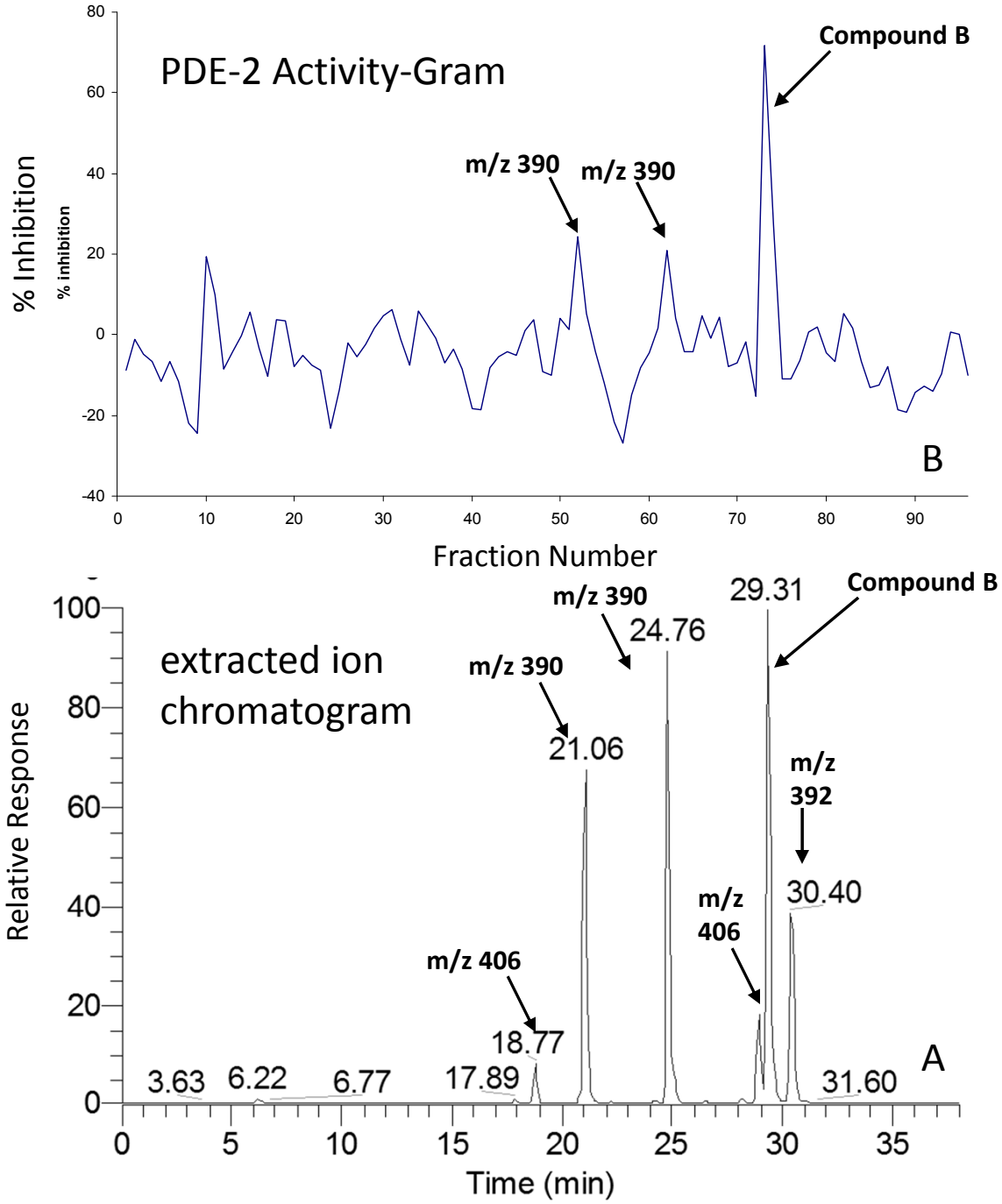

Figure 4

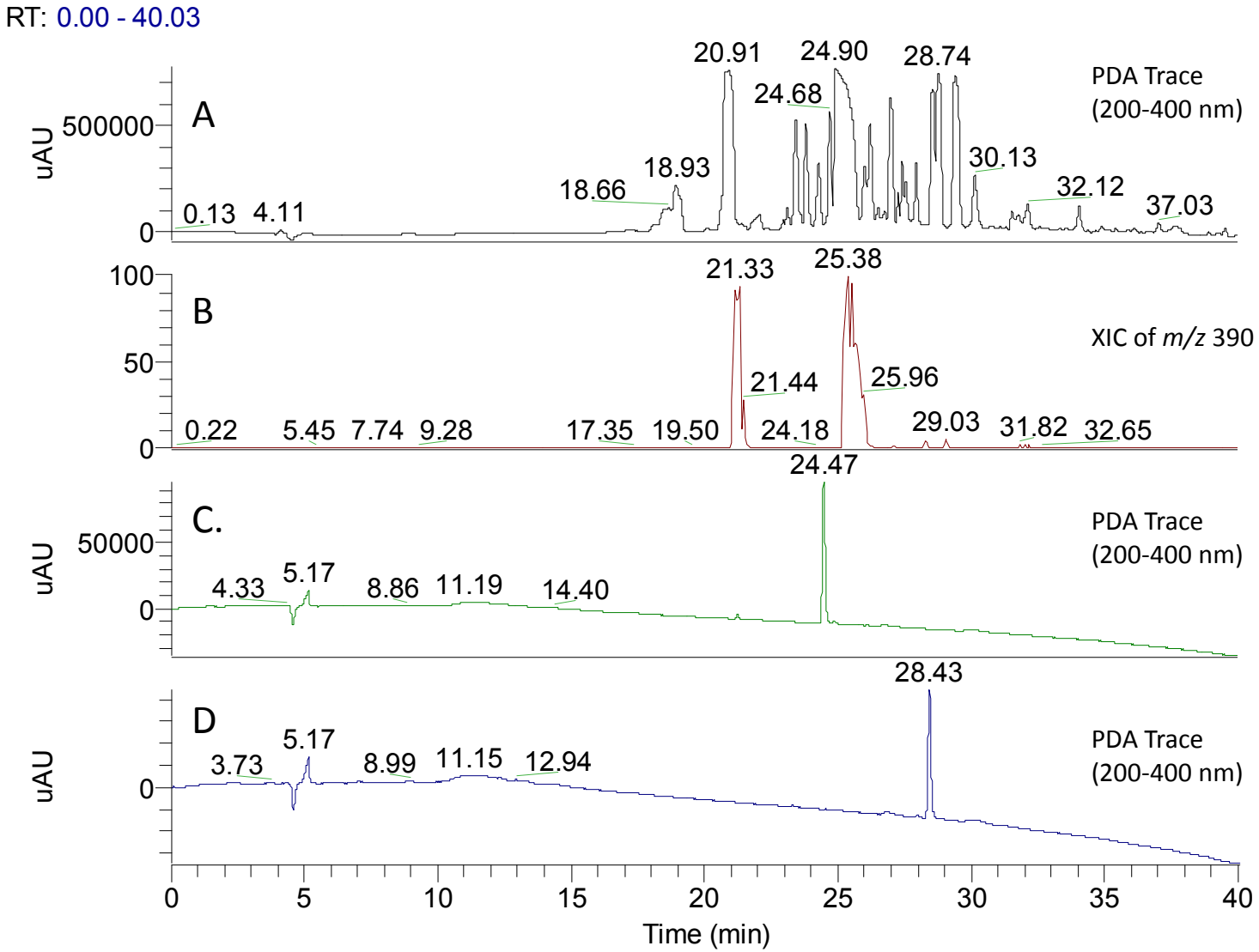

Figure 5

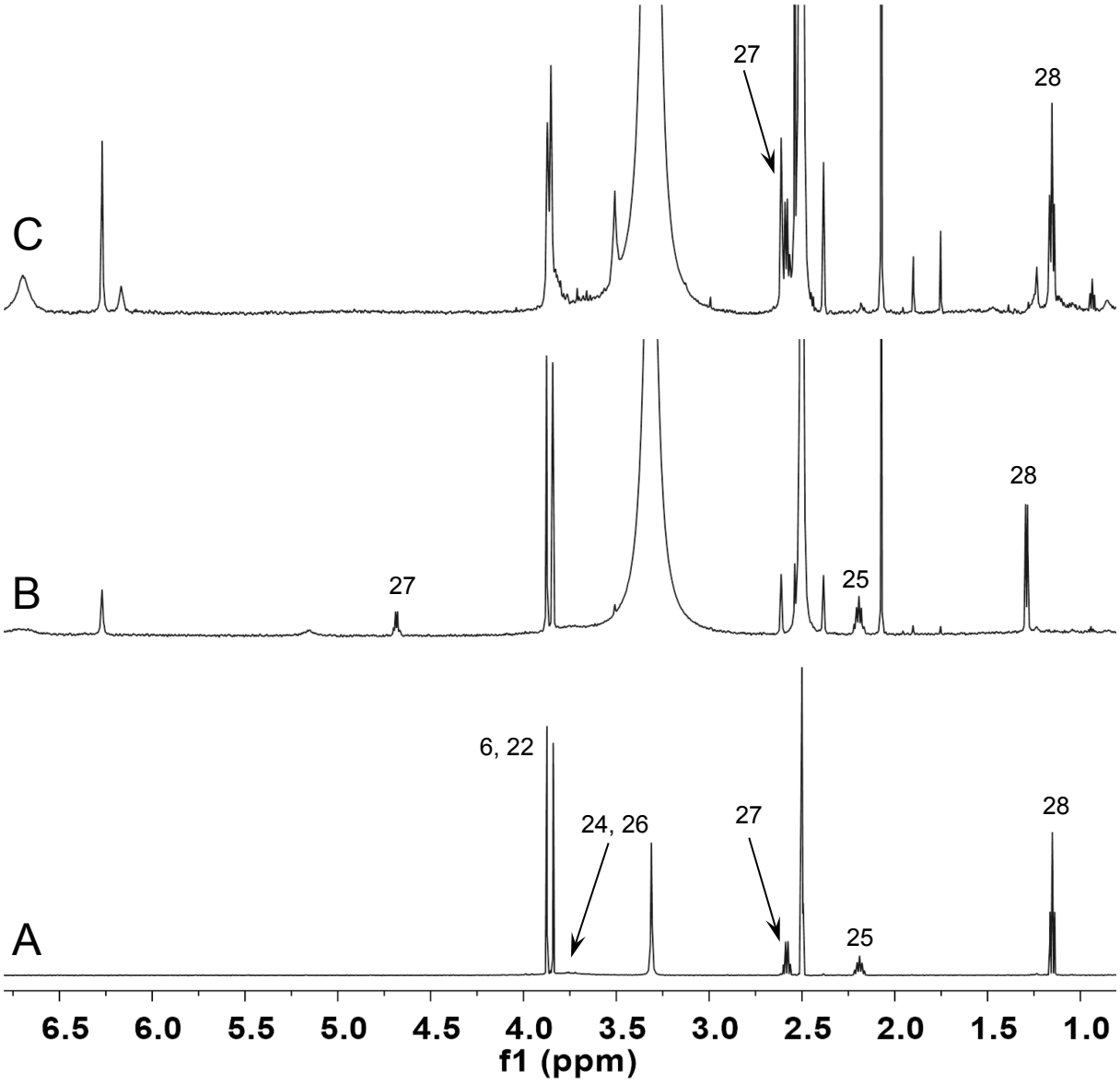

Figure 6

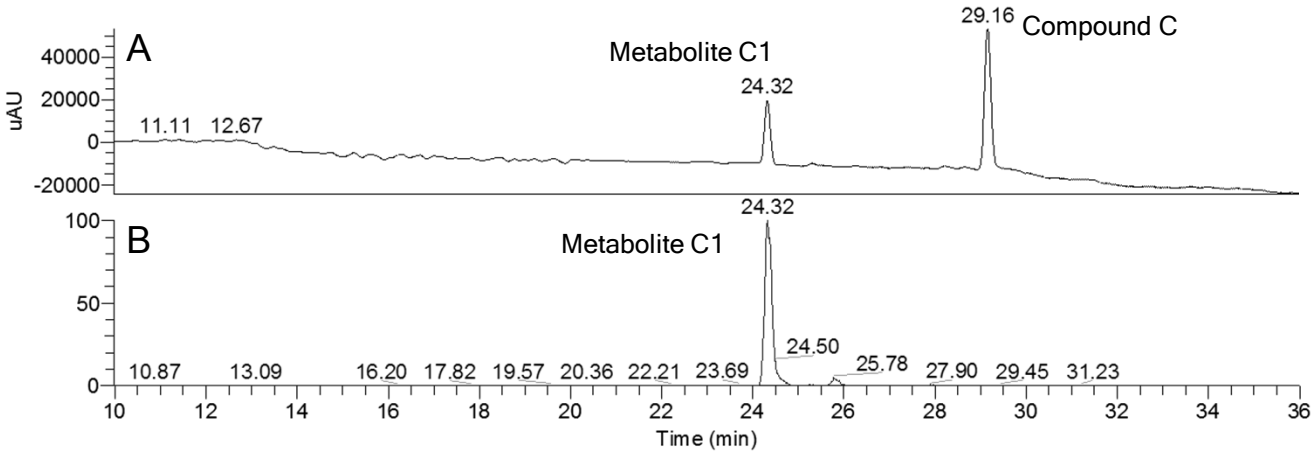

Figure 7

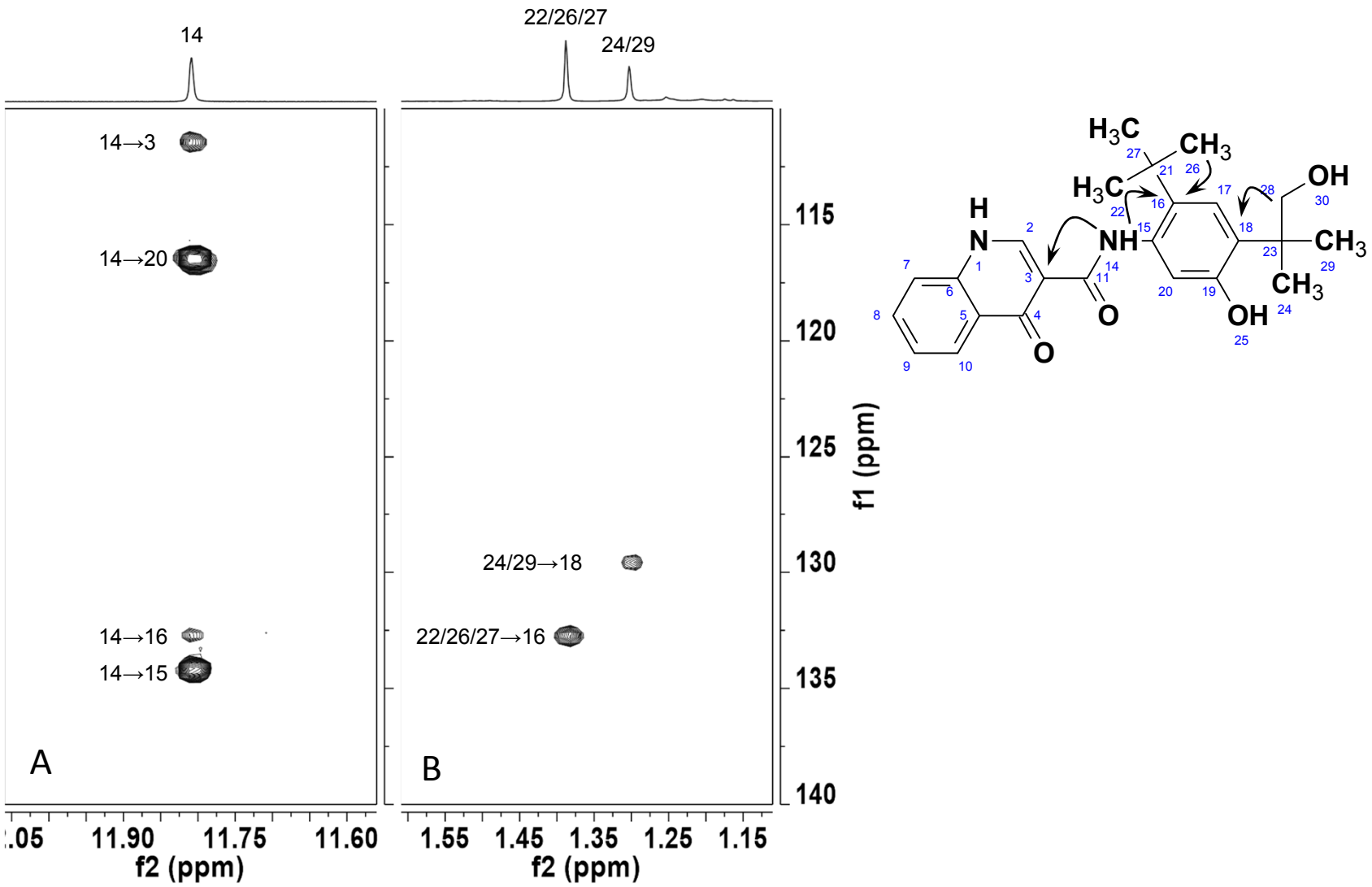

Figure 8

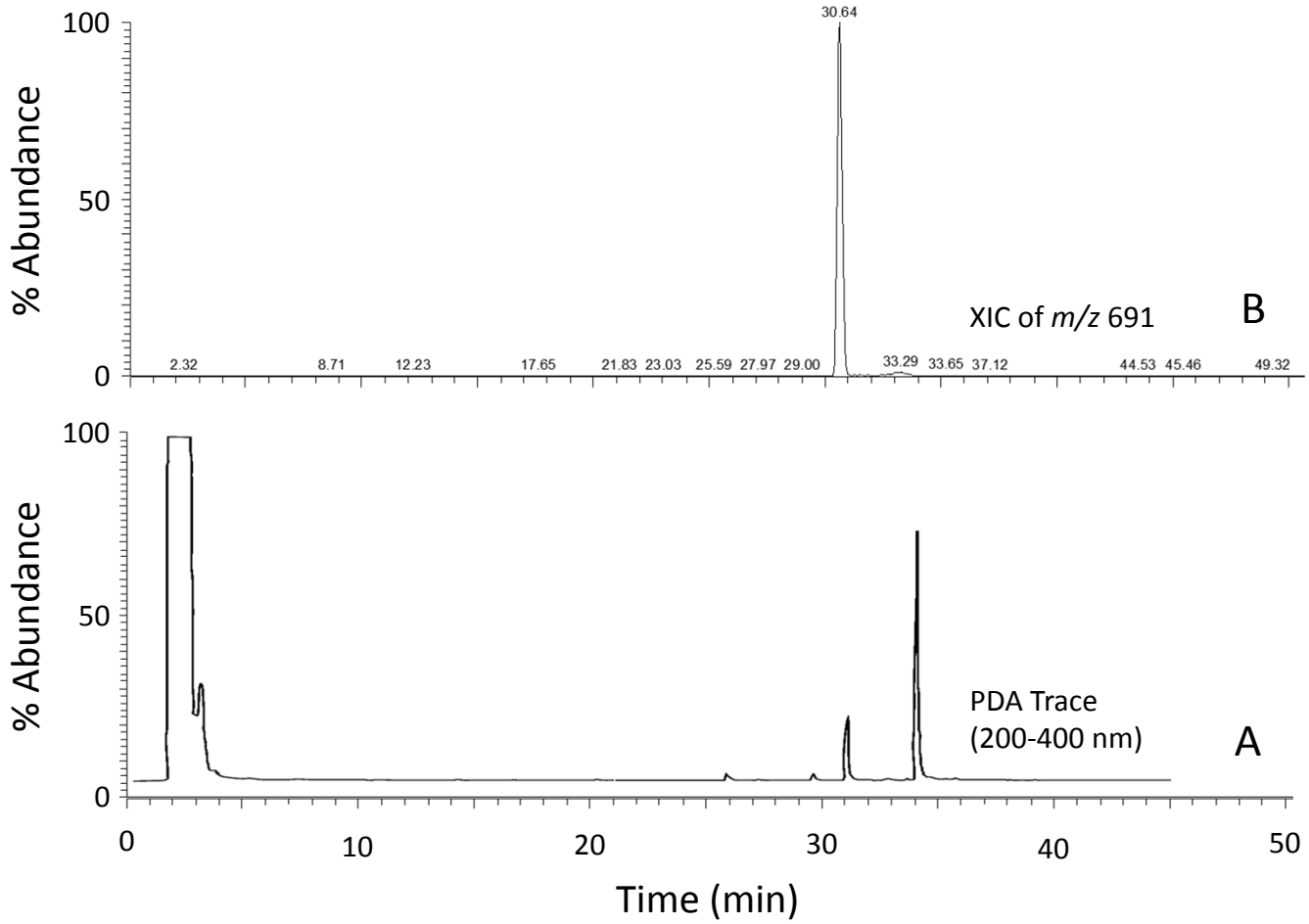

Figure 9

DMD Fast Forward. Published on July 22, 2014 as DOI: 10.1124/dmd.114.059204
This article has not been copyedited and formatted. The final version may differ from this version.

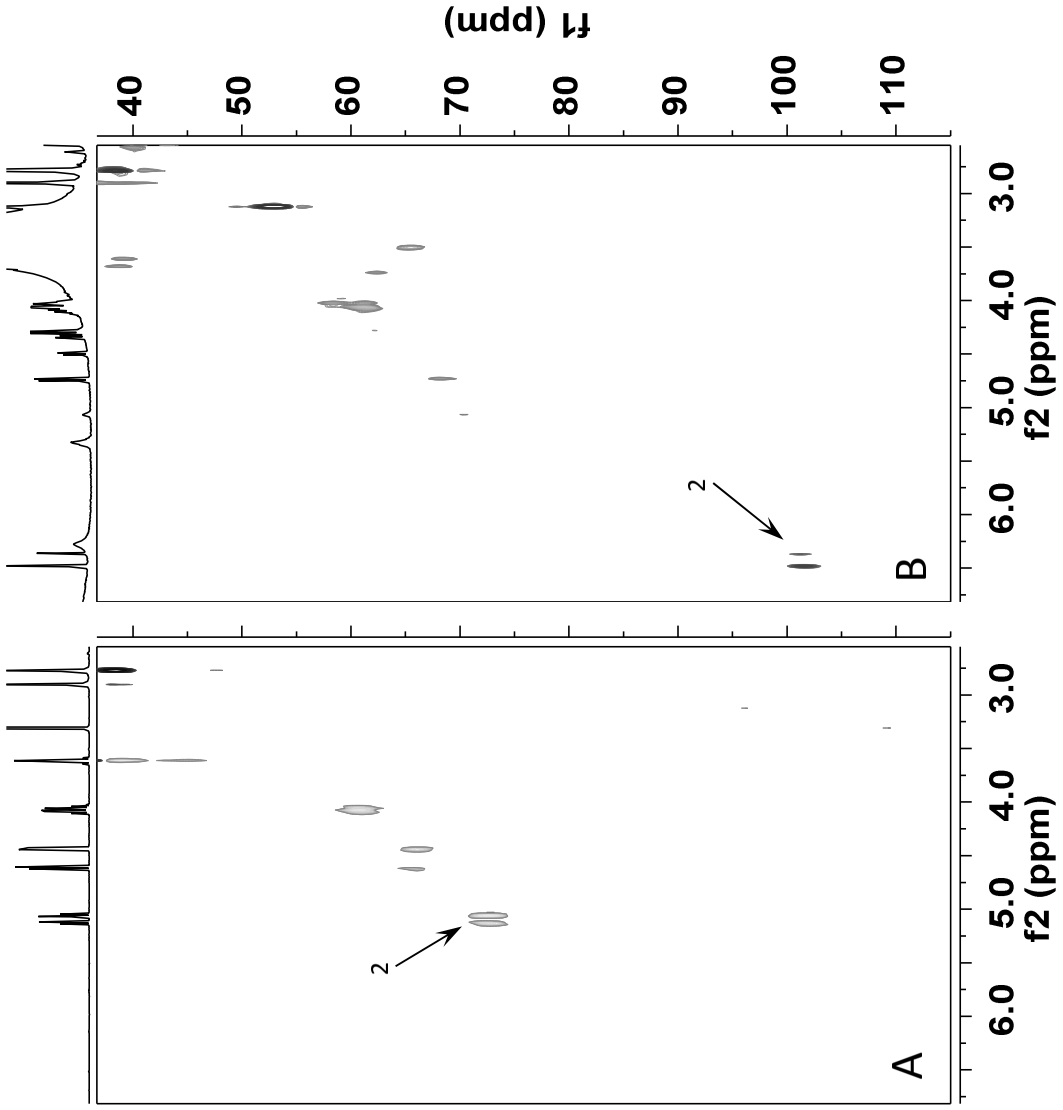

Figure 10

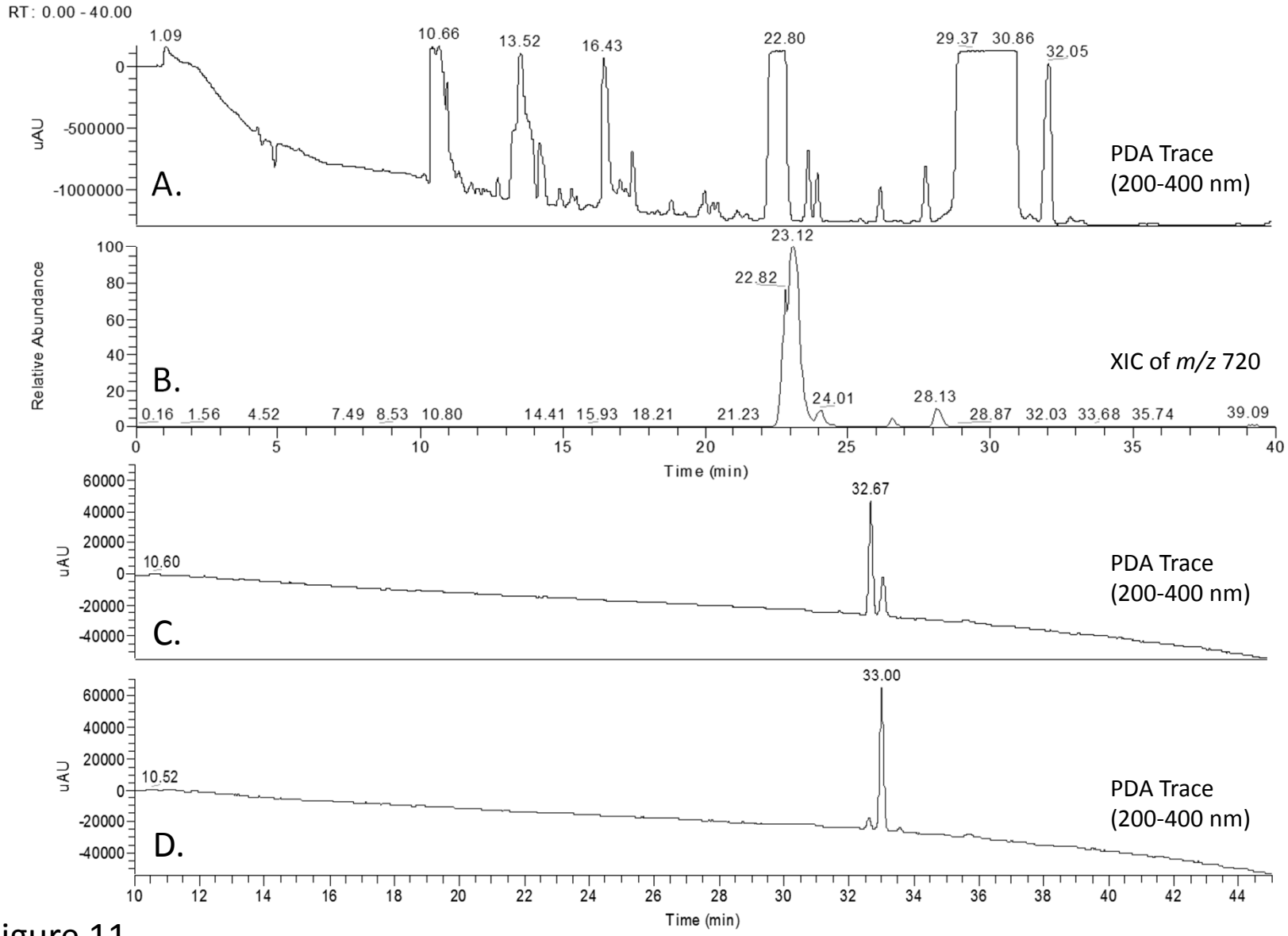

Figure 11

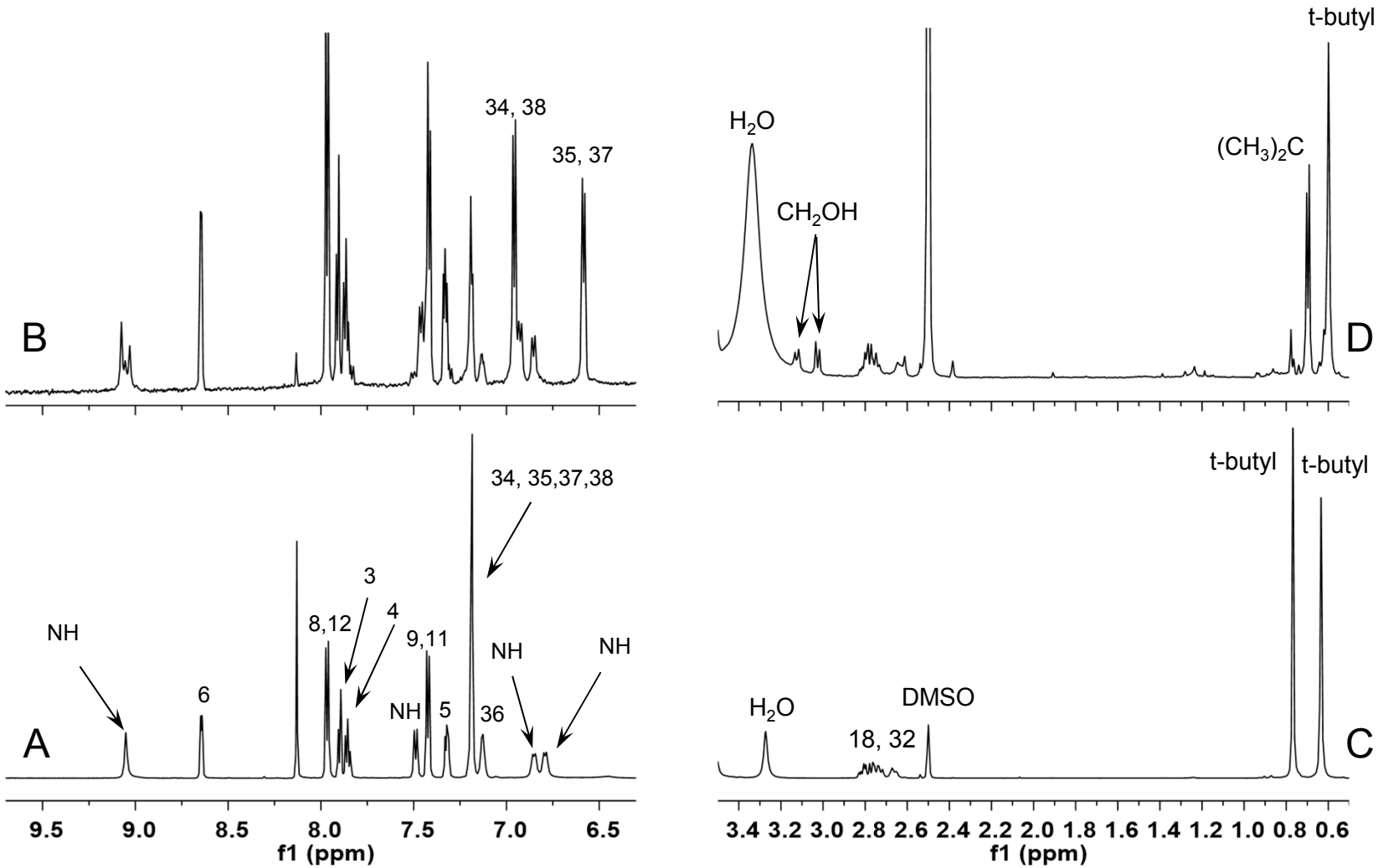

Figure 12

Drug Metabolism and Disposition

BIOSYNTHESIS OF DRUG METABOLITES AND QUANTITATION USING NMR SPECTROSCOPY FOR USE IN PHARMACOLOGICAL AND DRUG METABOLISM STUDIES

Gregory S. Walker, Jonathan N. Bauman, Tim F. Ryder, Evan B. Smith, Douglas K. Spracklin, and R. Scott Obach

Supplemental Data

Atazanavir MS^n Data

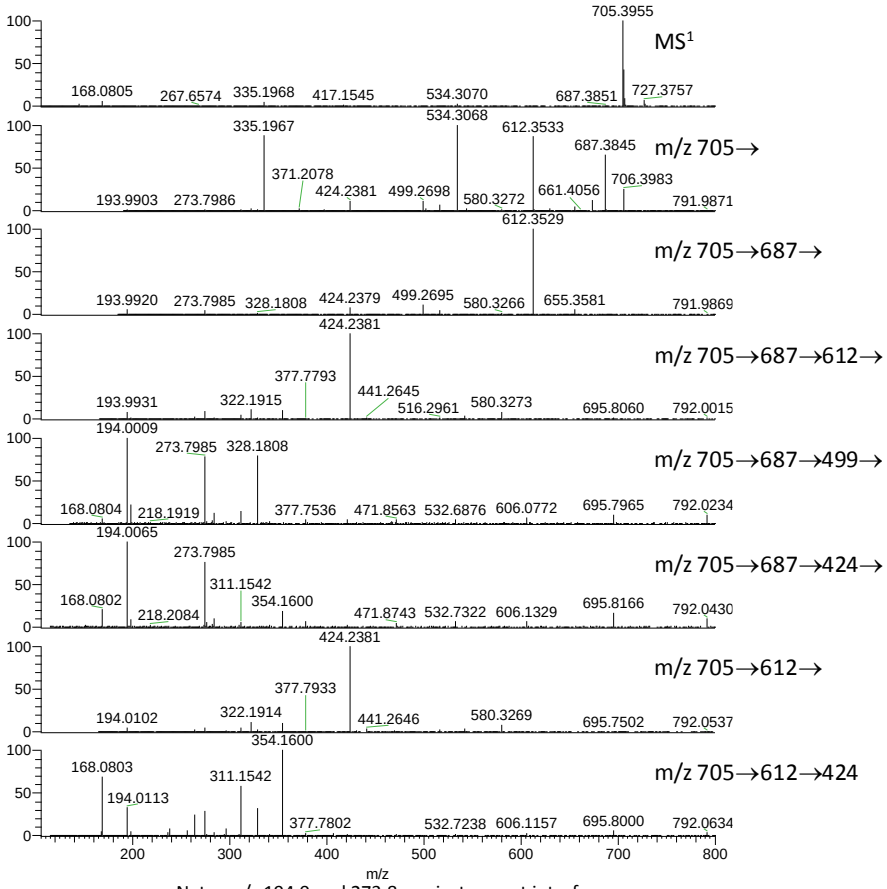

Note: m/z 194.0 and 273.8 are instrument interferences

Supplemental Figure 1
High Resolution Mass Spectrum of Atazanavir

Ion (m/z)	Formula	ppm
705.3955	$C_{38}H_{53}O_7N_6$	-2.3
687.3845	$C_{38}H_{51}O_6N_6$	-3.0
612.3533	$C_{36}H_{46}O_4N_5$	-1.8
580.3273	$C_{35}H_{42}O_3N_5$	-1.6
534.3068	$C_{30}H_{40}O_4N_5$	-1.3
499.2695	$C_{30}H_{35}O_3N_4$	-1.7
484.2698	$C_{29}H_{34}O_2N_5$	-1.9
424.2381	$C_{28}H_{30}ON_3$	-0.6
354.1600	$C_{23}H_{20}ON_3$	-0.3
335.1967	$C_{18}H_{27}O_4N_2$	0.5
328.1808	$C_{22}H_{22}N_3$	-0.1
322.1915	$C_{20}H_{24}ON_3$	0.3
311.1542	$C_{22}H_{19}N_2$	-0.2
298.1589	$C_{22}H_{20}N$	-0.4
250.1072	$C_{13}H_{16}O_4N$	-0.7
168.0803	$C_{12}H_{10}N$	-2.8
144.1015	$C_7H_{14}O_2N$	-0.7
112.0753	$C_6H_{10}ON$	-3.5

Supplemental Figure 1
(continued)

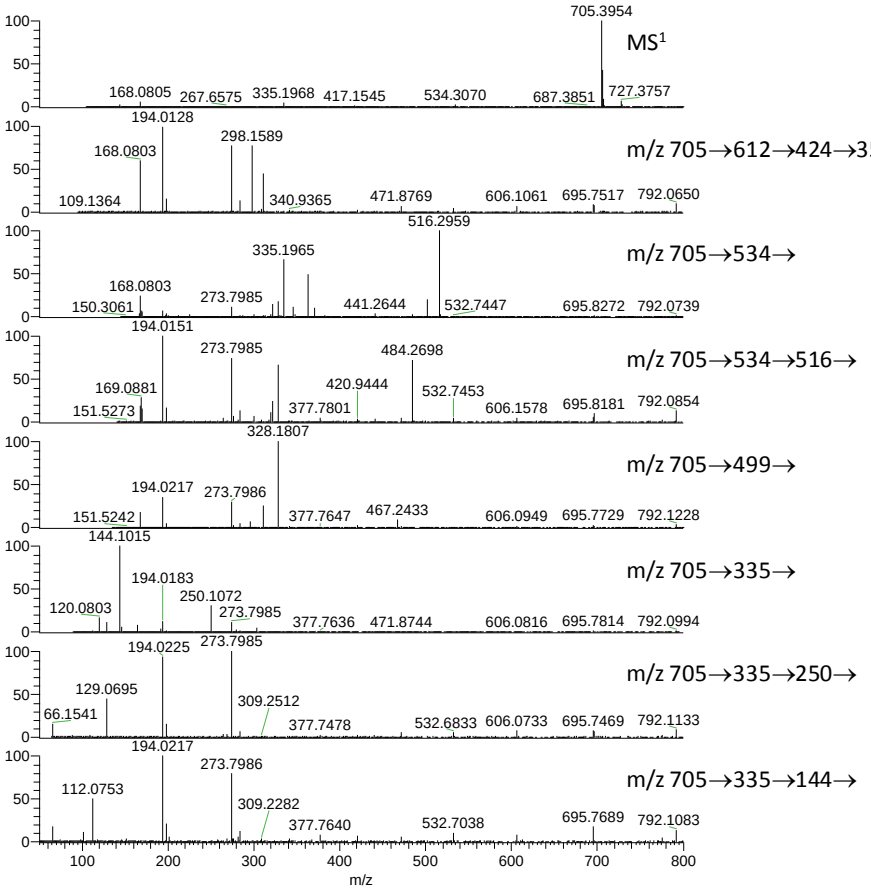

Note: m/z 194.0 and 273.8 are instrument interferences

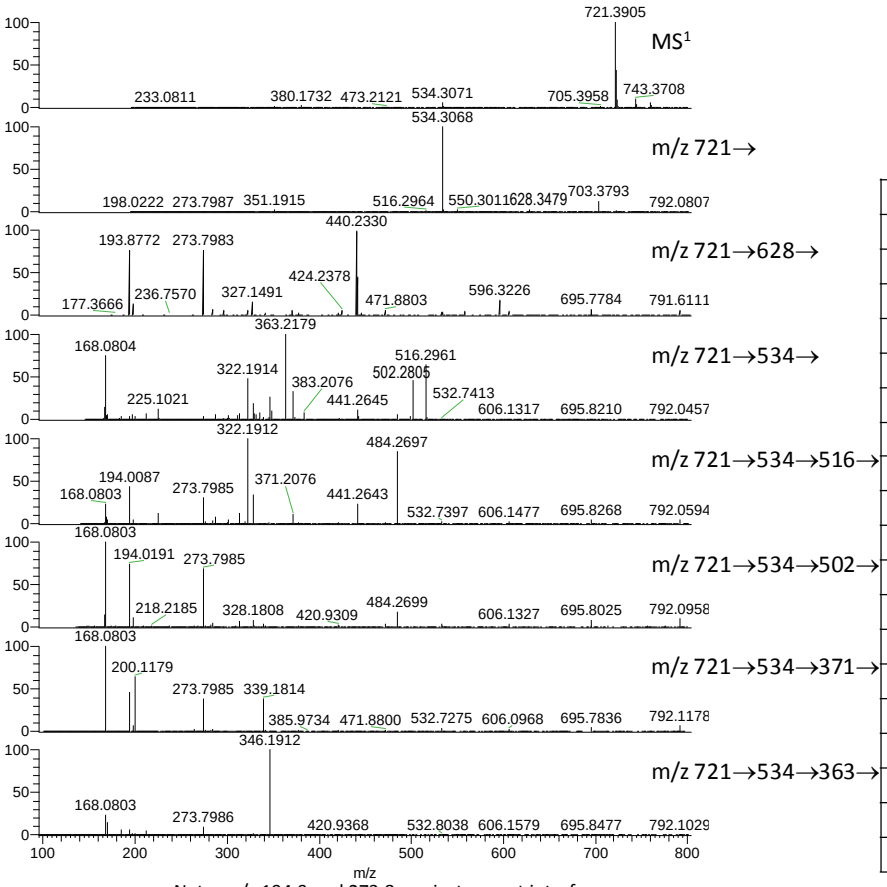

Note: m/z 194.0 and 273.8 are instrument interferences

Supplemental Figure 2 High Resolution Mass Spectrum of t-Butyl Hydroxyatazanavir

Ion (m/z)	Formula	ppm
721.3905	$C_{38}H_{53}O_8N_6$	-2.0
703.3793	$C_{38}H_{51}O_7N_6$	-2.9
628.3479	$C_{36}H_{46}O_5N_5$	-2.3
534.3068	$C_{30}H_{40}O_4N_5$	-1.3
516.2961	$C_{30}H_{38}O_3N_5$	-1.5
502.2805	$C_{29}H_{36}O_3N_5$	-1.5
484.2697	$C_{29}H_{34}O_2N_5$	-2.0
440.2330	$C_{28}H_{30}O_2N_3$	-0.6
371.2076	$C_{20}H_{27}O_3N_4$	-0.5
363.2179	$C_{22}H_{27}ON_4$	-0.1
351.1915	$C_{18}H_{27}O_5N_2$	0.2
346.1912	$C_{22}H_{24}ON_3$	-0.5
339.1814	$C_{19}H_{23}O_2N_4$	-0.5
322.1912	$C_{20}H_{24}ON_3$	-0.6
225.1020	$C_{14}H_{13}ON_2$	-1.0
200.1179	$C_{12}H_{14}N_3$	-1.6
170.0959	$C_{12}H_{12}N$	-3.1
168.0803	$C_{12}H_{10}N$	-2.8
164.1065	$C_{10}H_{14}ON$	-3.0

Supplemental Figure 2
(continued)

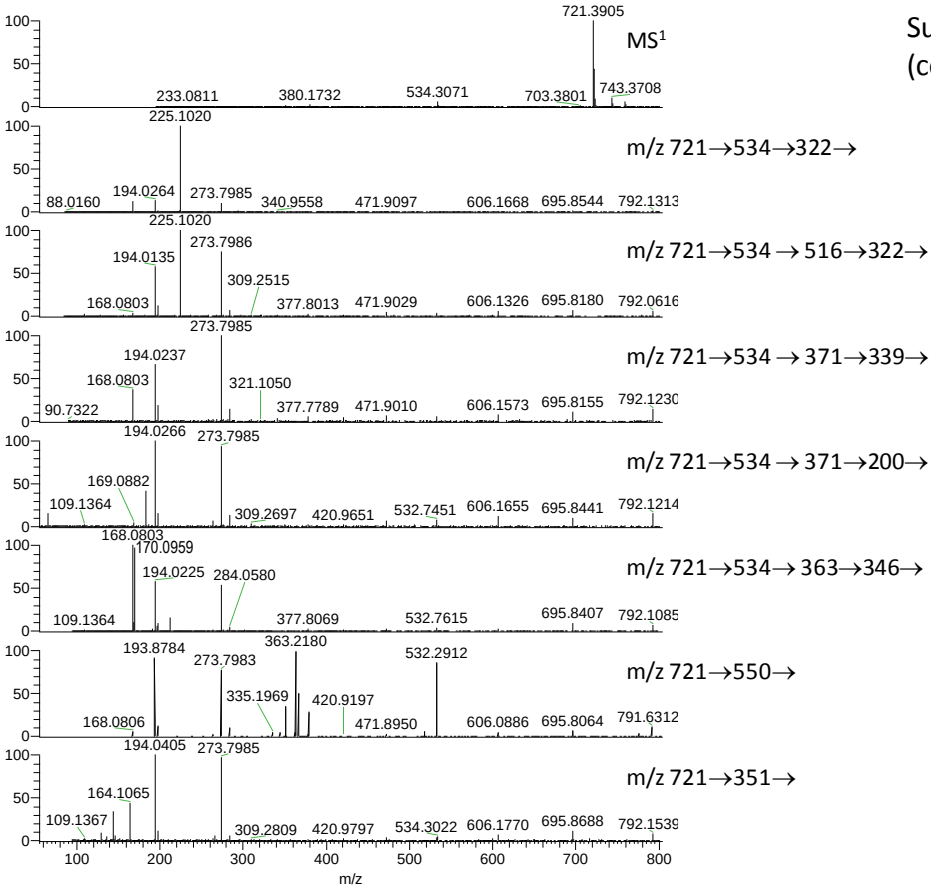

Note: m/z 194.0 and 273.8 are instrument interferences

Figure 3

Supplemental Figure 3

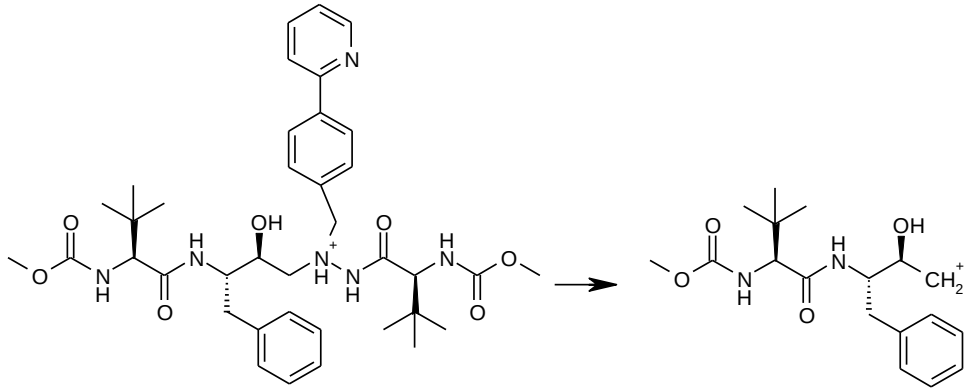

atazanavir (m/z 705.3955)

m/z 335.1967

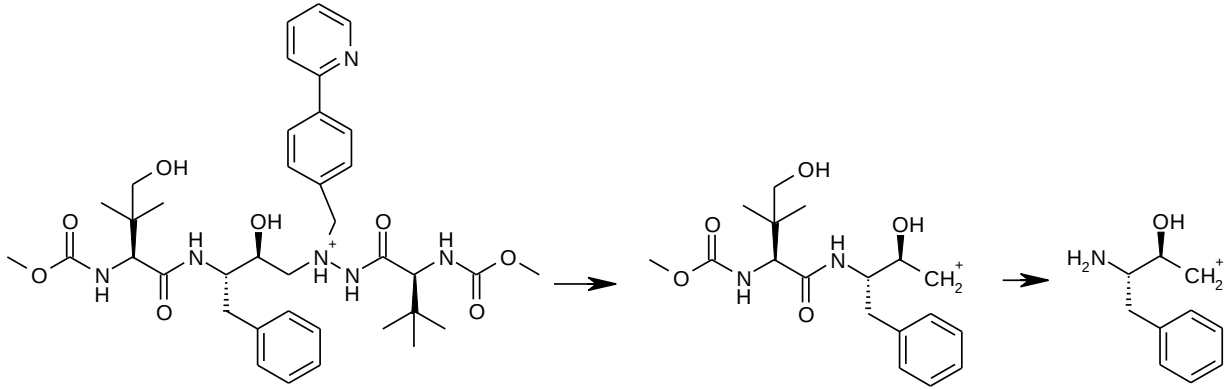

t-butyl hydroxyatazanavir (m/z 721.3905)

m/z 351.1915

m/z 164.1065

Figure 4A

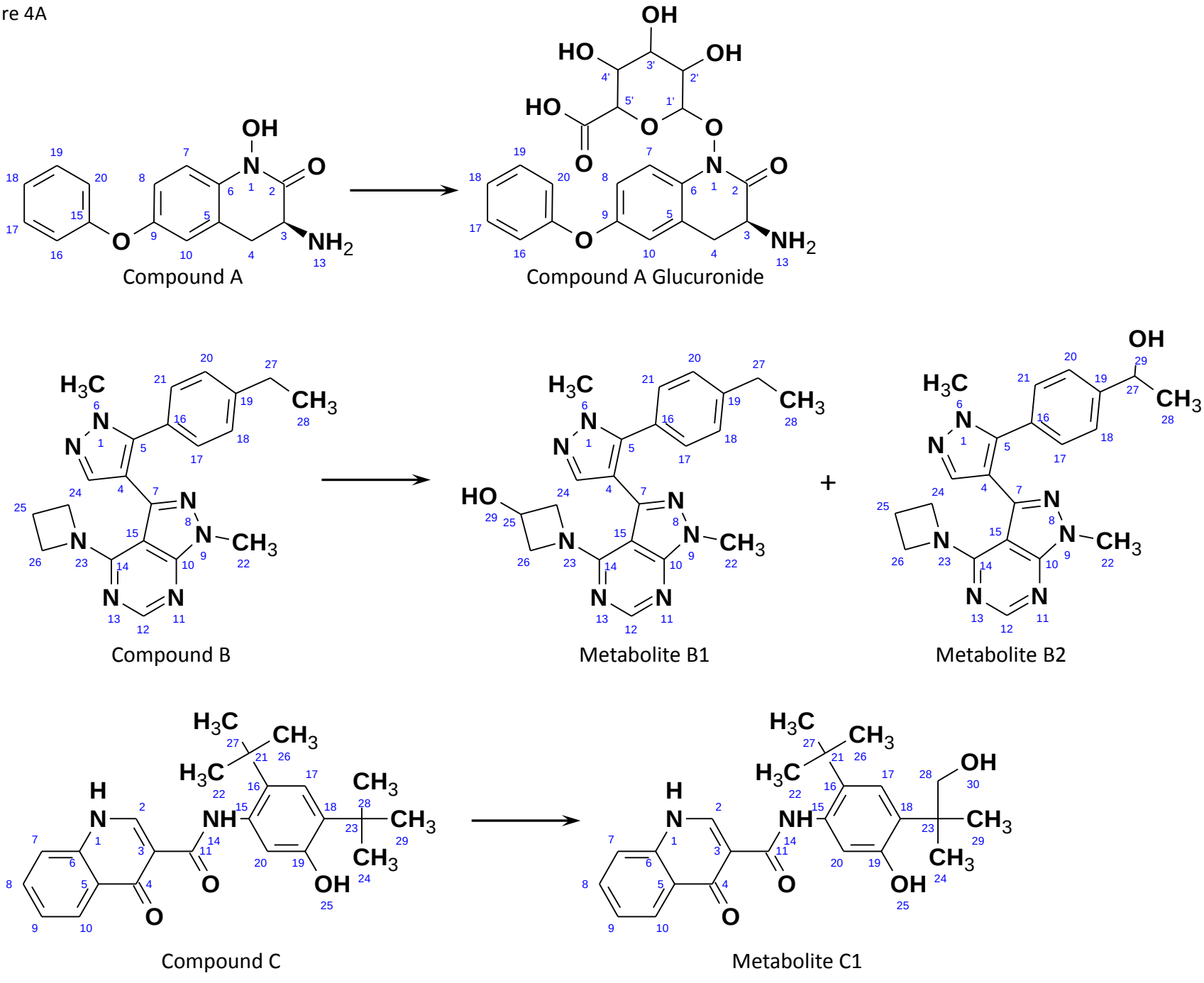
Compound A
Compound A Glucuronide
Compound B
Metabolite B1
Metabolite B2
Compound C
Metabolite C1

Figure 4B

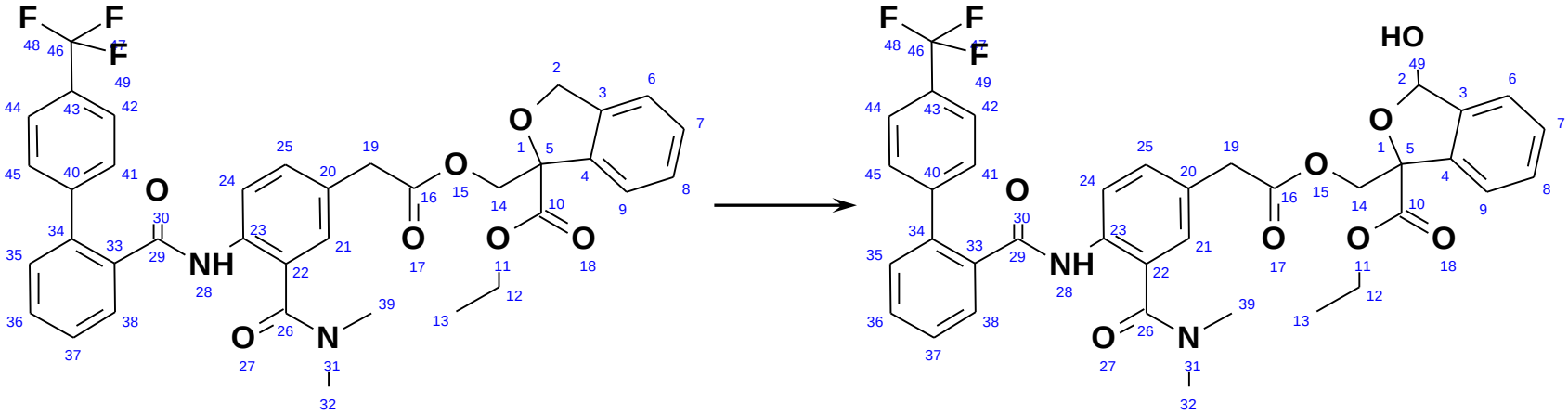

Compound D

Metabolite D1

Figure 4C